U.S. Department of Transportation

Federal Railroad Administration

Fire Performance of a UN-T75 Portable Tank Phase 1: Loaded with Liquid Nitrogen

Office of Research,
Development
and Technology
Washington, DC 20590

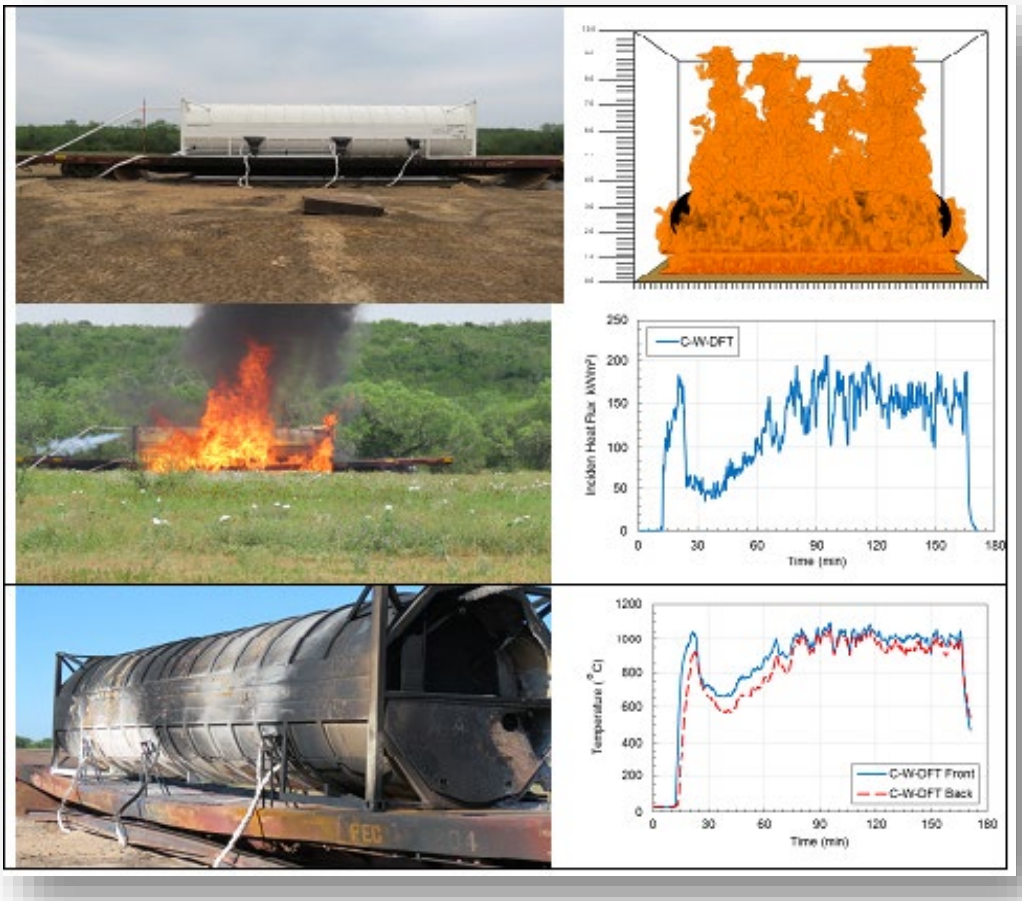

DOT/FRA/ORD-20/02

Final Report
January 2020

NOTICE

This document is disseminated under the sponsorship of the Department of Transportation in the interest of information exchange. The United States Government assumes no liability for its contents or use thereof. Any opinions, findings and conclusions, or recommendations expressed in this material do not necessarily reflect the views or policies of the United States Government, nor does mention of trade names, commercial products, or organizations imply endorsement by the United States Government. The United States Government assumes no liability for the content or use of the material contained in this document.

NOTICE

The United States Government does not endorse products or manufacturers. Trade or manufacturers' names appear herein solely because they are considered essential to the objective of this report.

REPORT DOCUMENTATION PAGE

Form Approved
OMB No. 0704-0188

Public reporting burden for this collection of information is estimated to average 1 hour per response, including the time for reviewing instructions, searching existing data sources, gathering and maintaining the data needed, and completing and reviewing the collection of information. Send comments regarding this burden estimate or any other aspect of this collection of information, including suggestions for reducing this burden, to Washington Headquarters Services, Directorate for Information Operations and Reports, 1215 Jefferson Davis Highway, Suite 1204, Arlington, VA 22202-4302, and to the Office of Management and Budget, Paperwork Reduction Project (0704-0188), Washington, DC 20503.

1. AGENCY USE ONLY (Leave blank)	2. REPORT DATE	3. REPORT TYPE AND DATES COVERED
	January 2020	Technical Report, September 2016–August 2017

4. TITLE AND SUBTITLE
Fire Performance of a UN-T75 Portable Tank Phase 1: Loaded with Liquid Nitrogen

5. FUNDING NUMBERS
Contract DTFR53-16-C-00017

6. AUTHOR(S)
Jason Huczek, Matthew Blais, and Keith Friedman

7. PERFORMING ORGANIZATION NAME(S) AND ADDRESS(ES)
Southwest Research Institute (SwRI)
6220 Culebra Road, Bldg. 143
San Antonio, TX 78238

Freidman Research Corporation (FRC)
1508-B Ferguson Lane
Austin, TX 78754

8. PERFORMING ORGANIZATION REPORT NUMBER
01.22307.01.006

9. SPONSORING/MONITORING AGENCY NAME(S) AND ADDRESS(ES)
U.S. Department of Transportation
Federal Railroad Administration
Office of Railroad Policy and Development
Office of Research, Development and Technology
Washington, DC 20590

10. SPONSORING/MONITORING AGENCY REPORT NUMBER
DOT/FRA/ORD-20/02

11. SUPPLEMENTARY NOTES
COR: Francisco González, III

12a. DISTRIBUTION/AVAILABILITY STATEMENT
This document is available to the public through the FRA website.

12b. DISTRIBUTION CODE

13. ABSTRACT (Maximum 200 words)
Southwest Research Institute (SwRI) fire-tested a portable tank (filled with liquid nitrogen [LN2]) and observed the demonstration of the performance of the pressure relief valve system in this Phase 1 project. In addition, several types of data have been collected during the experiment to understand how the fire exposure affects the internal and external heating of the tank. This information will be used in future computer modeling efforts to predict performance with different tanks and fire scenarios. The next phase of the project will include an additional test, with the test tank filled with liquefied natural gas (LNG) instead of LN2. The results of the second test will be compared to the first test and will also provide additional validation data for future modeling calculations.

14. SUBJECT TERMS
Liquefied natural gas, LNG, liquid nitrogen, LN2, ISO UN-T75 tank, flatcar, pressure relief valve, PRV, pressure relief device, PRD, directional flame thermometer, DFT, incident heat flux, surface temperature, hazardous materials

15. NUMBER OF PAGES
80

16. PRICE CODE

17. SECURITY CLASSIFICATION OF REPORT	18. SECURITY CLASSIFICATION OF THIS PAGE	19. SECURITY CLASSIFICATION OF ABSTRACT	20. LIMITATION OF ABSTRACT
Unclassified	Unclassified	Unclassified	

NSN 7540-01-280-5500
Standard Form 298 (Rev. 2-89)
Prescribed by ANSI Std. 239-18
298-102

METRIC/ENGLISH CONVERSION FACTORS

ENGLISH TO METRIC	METRIC TO ENGLISH
LENGTH (APPROXIMATE)	**LENGTH (APPROXIMATE)**
1 inch (in) = 2.5 centimeters (cm)	1 millimeter (mm) = 0.04 inch (in)
1 foot (ft) = 30 centimeters (cm)	1 centimeter (cm) = 0.4 inch (in)
1 yard (yd) = 0.9 meter (m)	1 meter (m) = 3.3 feet (ft)
1 mile (mi) = 1.6 kilometers (km)	1 meter (m) = 1.1 yards (yd)
	1 kilometer (km) = 0.6 mile (mi)
AREA (APPROXIMATE)	**AREA (APPROXIMATE)**
1 square inch (sq in, in^2) = 6.5 square centimeters (cm^2)	1 square centimeter (cm^2) = 0.16 square inch (sq in, in^2)
1 square foot (sq ft, ft^2) = 0.09 square meter (m^2)	1 square meter (m^2) = 1.2 square yards (sq yd, yd^2)
1 square yard (sq yd, yd^2) = 0.8 square meter (m^2)	1 square kilometer (km^2) = 0.4 square mile (sq mi, mi^2)
1 square mile (sq mi, mi^2) = 2.6 square kilometers (km^2)	10,000 square meters (m^2) = 1 hectare (ha) = 2.5 acres
1 acre = 0.4 hectare (he) = 4,000 square meters (m^2)	
MASS - WEIGHT (APPROXIMATE)	**MASS - WEIGHT (APPROXIMATE)**
1 ounce (oz) = 28 grams (gm)	1 gram (gm) = 0.036 ounce (oz)
1 pound (lb) = 0.45 kilogram (kg)	1 kilogram (kg) = 2.2 pounds (lb)
1 short ton = 2,000 pounds (lb) = 0.9 tonne (t)	1 tonne (t) = 1,000 kilograms (kg)
	= 1.1 short tons
VOLUME (APPROXIMATE)	**VOLUME (APPROXIMATE)**
1 teaspoon (tsp) = 5 milliliters (ml)	1 milliliter (ml) = 0.03 fluid ounce (fl oz)
1 tablespoon (tbsp) = 15 milliliters (ml)	1 liter (l) = 2.1 pints (pt)
1 fluid ounce (fl oz) = 30 milliliters (ml)	1 liter (l) = 1.06 quarts (qt)
1 cup (c) = 0.24 liter (l)	1 liter (l) = 0.26 gallon (gal)
1 pint (pt) = 0.47 liter (l)	
1 quart (qt) = 0.96 liter (l)	
1 gallon (gal) = 3.8 liters (l)	
1 cubic foot (cu ft, ft^3) = 0.03 cubic meter (m^3)	1 cubic meter (m^3) = 36 cubic feet (cu ft, ft^3)
1 cubic yard (cu yd, yd^3) = 0.76 cubic meter (m^3)	1 cubic meter (m^3) = 1.3 cubic yards (cu yd, yd^3)
TEMPERATURE (EXACT)	**TEMPERATURE (EXACT)**
[(x-32)(5/9)] °F = y °C	[(9/5) y + 32] °C = x °F

QUICK INCH - CENTIMETER LENGTH CONVERSION

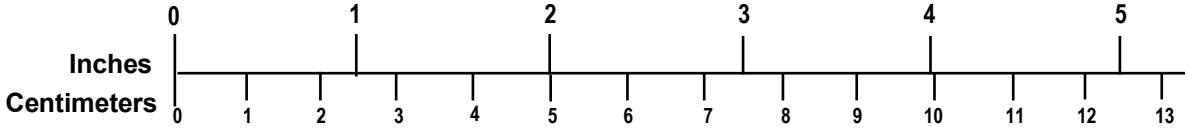

QUICK FAHRENHEIT - CELSIUS TEMPERATURE CONVERSIO

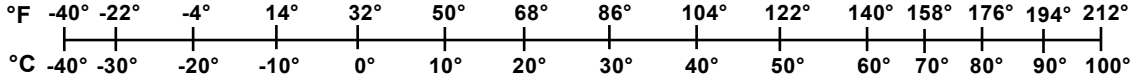

For more exact and or other conversion factors, see NIST Miscellaneous Publication 286, Units of Weights and Measures. Price $2.50 SD Catalog No. C13 10286

Updated 6/17/98

Acknowledgements

Southwest Research Institute (SwRI) and Freidman Research Corporation (FRC) would like to acknowledge Francisco González, III and Phani Raj at the Federal Railroad Administration (FRA) for their technical guidance throughout the first phase of this project.

Contents

Illustrations

Tables

Executive Summary

From September 2016 to August 2017, the Federal Railroad Administration contracted Southwest Research Institute (SwRI) to fire-test a portable tank (filled with liquid nitrogen [LN2]) and demonstrate the performance of the pressure relief valve (PRV) system installed on the tank. The PRVs opened and were able to relieve the pressure in the tank fast enough to avoid a Boiling Liquid Expanding Vapor Explosion (BLEVE) event. In addition, several types of data have been collected during the experiment to understand how the fire exposure affects the internal and external heating of the tank. This information will be used in future computer modeling efforts to predict performance with different tanks and fire scenarios.

The next phase of the project will include an additional test, like the fire test, but with the test tank filled with liquefied natural gas (LNG) instead of LN2. The results of the second test will be compared to the first test and will also provide additional validation data for future modeling calculations.

The railroad industry is actively working on alternative fuels to diesel, including LNG and Compressed Natural Gas (CNG). The safety performance of these alternate fuel tank cars under derailment induced fire conditions has not been verified and is a cause for concern. FRA is interested in methods and approaches, both analytical and experimental, which can evaluate the thermal safety performance of LNG/CNG means of containment under fire conditions.

In addition, the railroad industry is working on alternatives to diesel fuels in locomotives due to the potential reductions in greenhouse gas (GHG) emissions, fuel costs, and refueling times by using CNG or LNG fuels. Currently the rail industry spends about $9 billion on fuel costs. Two different tender design approaches are being considered by the Association of American Railroads (AAR) Natural Gas Fuel Tender Technical Advisory Group (TAG); (i) using a tank car based design—with the United States Department of Transportation's (DOT) 113 specification car as a model; and (ii) 40-foot portable tanks on flatcars (two of which can be placed back to back on a flatcar) CNG tender designs target switch or regional use. Design approaches that consider and protect the LNG tender from potential exposure to a pool fire are of interest. The potential effects of the design approaches under fire conditions are of interest.

The purpose of the first phase of this project was to conduct fire testing of a portable tank filled with LN2, located on top of a flat railcar and exposed to a propane pool fire.

The report provides additional detail of the test portable tank, the flatcar supporting the portable tank, the development of a safety plan, characterization of the fire exposure source and burning duration, description of the instrumentation used in the experiment, test results as well as preliminary modeling calculations.

The following conclusions related to the fire testing are provided:

- A portable tank, filled with LN2, was exposed to a liquefied petroleum gas (LPG) fire for 2 hours, 35 minutes.
- There was no rupture or BLEVE of either the inner or outer tank.
- The steel in the flatcar exceeded its softening temperature. The flatcar sagged downward until it was supported by the fire pan.

- Based on the internal pressure rise, the insulation degraded in the fire relatively quickly. It is expected that the thermal properties of the insulation material will greatly affect the performance of the tank in a fire scenario.
- The pressure inside the inner tank increased monotonically during the fire exposure and stabilized at approximately 180 psig.
- The PRV system worked properly. The lower pressure (114 psig) valve opened and reseated twice and then opened fully. The higher-pressure valve opened at about 150 psig. The pressure continued to rise until 180 psi and the venting stabilized.
- There was additional venting after the fire exposure stopped and this continued for more than 3 hours, 40 minutes—the extent of video footage after fire exposure finished.
- The next morning after the test, the internal pressure in the tank was nearly atmospheric, there was no visible venting of the remaining LN2 in the portable tank, and there was no vacuum in the annular space.
- The venting orientation/direction could be important in the field. The venting jet on this tank would impinge on a joining portable tank or rail car. If tested with LNG this vent would be like a torch and could spread the fire to neighboring tanks. This phenomenon will be able to be observed and evaluated in the next phase of this project.

The following conclusions related to the modeling are provided:

- The temperature of a tank will greatly influence the failure pressure of that tank. The failure pressure for a heated tank has been shown to be much less than that of a tank at ambient temperature.
- The preliminary modeling results suggest that additional effort should be applied to assessing the potential failure of the tank under elevated temperatures.
- The preliminary modeling results suggest that additional effort should be applied to accurately characterizing the thermal insulation properties as well as vacuum retention capabilities of the annular space under thermal loading.
- The introduction of phase change into the modeling needs to be accomplished to better understand the various mechanisms that are involved during the heating process.
- Studying the effect of wind, flatcar geometry, and burner size on the heat flux to the tank should be expanded so as to better understand the effects of conditions that may be present at the physical test.
- The results obtained in the test should be utilized to validate the models developed in the next phase of this project.

1. Introduction

The U.S. Department of Transportation's (DOT) Federal Railroad Administration (FRA) awarded a contract to Southwest Research Institute (SwRI) to conduct research and fire testing on a portable tank built in accordance with the United Nations (UN) T75 standards to carry cryogenic liquids such as liquefied natural gas (LNG). SwRI is submitting this report on the evaluation of fire performance of a portable tank UN-T75 using analytical methods and fire testing.

1.1 Background

The railroad industry is actively working on alternative fuels to diesel, including LNG and Compressed Natural Gas (CNG). The safety performance of these alternate fuel tenders under derailment induced fire conditions has not been verified and is a cause for concern. FRA is interested in methods and approaches, both analytical and experimental, which can evaluate the thermal safety performance of LNG/CNG means of containment (tanks, portable tanks, tenders, etc.) under fire conditions.

In addition, the railroad industry is working on alternatives to diesel fuels in locomotives due to the potential reductions in GHGs, fuel costs, and refueling times by using CNG or LNG fuels. Currently the rail industry spends about $9 billion on fuel costs. Two different tender design approaches are being considered by the Association of American Railroads (AAR) natural gas fuel Technical Advisory Group (TAG) using a tank car based design—with DOT 113 specification tank car as a model, and a 40-foot UN T75 portable tank on flatcars (two of which can be placed back to back on a flatcar). CNG tender designs target switch or regional use. Design approaches that consider and protect the LNG tender from potential exposure to a pool fire are of interest. The potential effects of the design approaches under fire conditions are of interest.

1.2 Objectives

The objective of Phase 1 of this project was to conduct fire testing of an ISO tank filled with LN2, located on top of a flat rail car and exposed to a propane pool fire, and evaluate the pressure relief valve system.

1.3 Overall Approach

A portable tank, for shipment by rail, has been exposed to fire conditions and the performance of the pressure relief valve (PRV) system has been observed. Additionally, collection of several types of data took place during the experiment to understand how the fire exposure affects the internal and external heating of the tank. This information will be used in future computer modeling efforts to predict performance with different tanks and fire scenarios.

1.4 Scope

SwRI fire-tested a portable tank, filled with liquid nitrogen (LN2), and demonstrated the performance of the PRV system. In addition, data was collected to understand how the fire

exposure affects the survivability of the portable tank. The next phase of the project will include an additional test, similar to the first test, but with the test tank filled with LNG instead of LN2.

1.5 Organization of the Report

Section 2 provides additional detail of the test tank and the flatcar supporting the tank; Section 3 details the development of a safety plan, while Section 4 offers the characterization of the fire exposure source and burning duration; Section 5 describes the instrumentation used in the experiment; Section 6 and Section 7 provides test results as well as preliminary modeling calculations, while Section 8 provides a conclusion, and Section 9 describes future work. Appendix A and B provide additional illustrations.

2. Test Articles

Two primary test articles were procured for this project. The first was the ISO UN-T75 storage tank and the second was the flatcar. The following sections provide additional details about these test articles.

2.1 LNG ISO Test Tank

An ISO UN-T75 storage tank, outfitted for LNG service, was procured from Cryogenic Vessel Alternatives, Inc. (CVA). The model number of the tank is CVA-12K-114-ISO and measures 40 feet long, 8.5 feet high and 8 feet wide. Figure 1 provides selected photographs of the tank that was used in this experiment. Additional figures can be referenced in Appendix A of this report.

Figure 1. ISO Test Tank Photographs

The test tank was filled with 7,047 gal (approximately 21,456 kg) of LN2, by Cryogenic Products, Inc. on May 8–9, 2017. Since the tank was fabricated for LNG use and LN2 is denser than LNG, the tank was under-filled with LN2 in order to not exceed the weight rating.

Various material properties for LN2 are listed below per the Airgas safety data sheet.

- Molecular weight: 28.01 g/mole
- Boiling/condensation point: -195.8 °C (-384.4 °F)
- Melting/freezing point: -210 °C (-346 °F)
- Critical temperature: -146.9 °C (-232.5 °F)

- Liquid density at boiling point: 808.3 kg/m^3 (50.46 lb/ft^3)
- Solubility in water: 0.023 g/l (0.0014 lb/ft^3)

2.2 Flatcar for ISO Tank Installation

FRA identified a project partner in the Florida East Coast Railway (FECR), that donated two flatcars connected together, in order to safely travel across the country by rail. Only one of these cars was utilized for the fire testing. The car was taken off the rail line at the Transload Operations location for Hondo Railway. The cars were disconnected and transported by truck to the remote test site, located in Sabinal, TX. Figure 2 shows two photographs of the flatcar prior to arrival at the remote site.

Figure 2. Flatcar Photographs (provided by FECR)

3. Safety Plan Development

SwRI submitted a test plan under SwRI Project number 01.22307.01.003, which provided the technical details concerning the safety plan. Several of those items are summarized again in the following sections.

3.1 LNG vs LN2 in ISO Tank

Based on the summarized historical data, in-house calculations and consultation with SwRI's safety department, it was decided to perform this test with LN2 in the test tank. Based on the results of this first test, the next test is planned to be conducted with LNG inside the test tank.

3.2 Review of Test Plan Safety Design

The following subsections provide additional details about the test plan safety design.

3.2.1 Historical Events

Historical events were reviewed and the standoff distance parameters were previously discussed for those events. There were two primary events in the last 15 years, where a large LNG tank failed catastrophically.

It should be noted that the tank designs for these two events were different from the design tested in this project. However, due to the lack of other available data, these events were as follows:

3.2.2 Tivissa, Catalonia, Spain

On June 22, 2002, an LNG tanker exploded in Tivissa, Catalonia, Spain. Results from the accident investigation have been published[1] and are summarized below.

- Overpressure
  - Investigators calculated the explosion with an equivalent mass of 66 lbs of trinitrotoluene (TNT)
- Sound Pressure Level
  - ~122 decibel level (dBA) at SwRI remote site fence line, based on estimated overpressure
- Shrapnel
  - Tank front end = 410 feet away, tank back end = 262 feet away
- Fireball
  - Radius = 246 feet, height = 371 feet, duration = 12 seconds

[1] Planas-Cuchi, Eulàlia, Núria Gasulla, Albert Ventosa, and Joaquim Casal. "Explosion of a Road Tanker Containing Liquefied Natural Gas," Journal of Loss Prevention in the Process Industries 17 (2004): 315–321.

- Estimated heat flux of 16 kW/m^2 at 650 feet (two bystanders received 1st and 2nd degree burns)

3.2.3 Murcia (Spain)

On October 20, 2011, an LNG tanker exploded in Murcia, Spain. Results from the accident investigation have been published and are summarized below:[2,3]

- Overpressure
  - Investigators calculated the explosion had an equivalent weight of 90 lbs TNT
  - Hill on one side of the explosion reflected the overpressure wave toward a gasoline station
- Sound Pressure Level
  - ~123 dBA at SwRI Remote Site fence line, based on estimated overpressure
- Shrapnel
  - Secondary fragments up to 656 feet
- Fireball
  - Radius = 218–258 feet, height = 328 feet, duration = 9.4 seconds
  - Estimated heat flux of 55 kW/m2 at a distance of 300 feet (pine needle pyrolysis)

3.2.4 Overpressure and Sound Pressure Level

Typical overpressure limits for structures and humans can be referenced in the Society of Fire Protection Engineers (SFPE) Handbook.[4] The limit utilized at the SwRI remote test site is 0.1 psig, which is nominally equivalent to typical window glass breakage.

The Occupational Safety and Health Administration (OSHA) sound pressure level exposure limits are as follows:

- PEL is 80 dB TWA for 8 hours
  - PEL = permissible exposure limit
  - TWA = time-weighted average
    - PEL is 115 dB for impulse noises (< 30 s)
    - Threshold of pain is 140 dB

[2] Martinez, Juan Manuel Bonilla, "Liquefied Natural Gas Road Tanker Explosion," Internal Report, Murcia Fire Service & Rescue, October 2011.
[3] Planas, E. et al., "Analysis of the BLEVE of a LNG road tanker: The Zarzalico accident," Journal of Loss Prevention in the Process Industries 34 (2015): 127–138.
[4] Hurley, M. et.al., "SFPE Handbook of Fire Protection Engineering, 5th Edition, Chapter 71: BLEVES and Fireballs," pp. 2806–2807, doi: 10.1007/978-1-4939-2565-0_71, Society of Fire Protection Engineers, 2016

The expected sound pressure levels can be calculated as a function of distance for varying amounts of overpressure, expressed as TNT equivalency.[5] This TNT input was taken from the historical event data described in more detail below.

Figure 3 shows a curve for 70- and 90-lb. TNT equivalent and the dBA and noise reduction rating (NRR), or dBA after accounting for hearing protection. It can be seen that onsite structures and personnel were able to be protected to a safe level in the event of a tank failure.

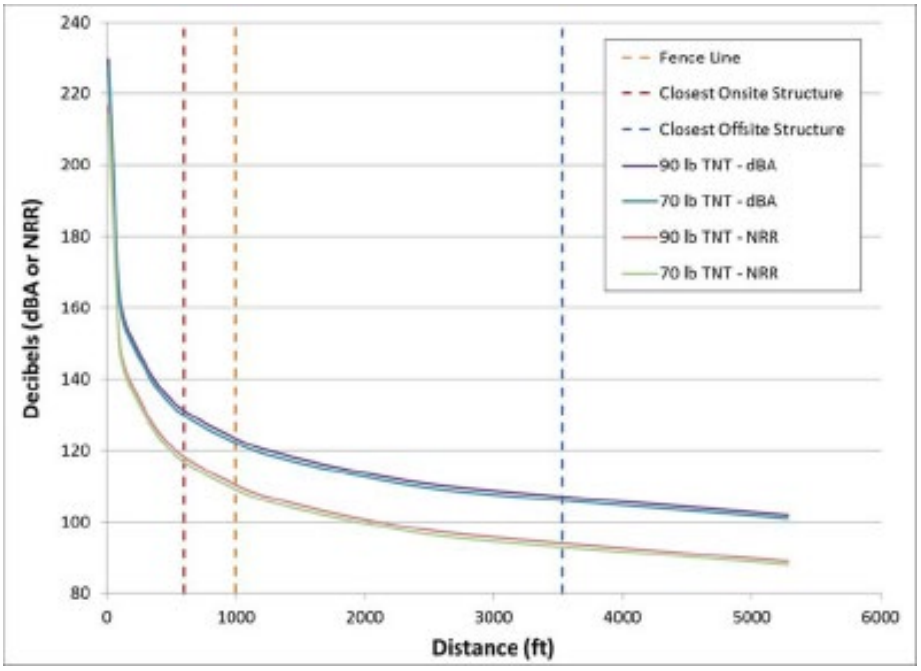

Figure 3. Calculated Sound Pressure Levels for Varying Overpressures

3.2.5 Shrapnel

It was necessary to plan for the possibility of shrapnel, if the tank failed catastrophically. The safety plan incorporated measures to protect people, equipment and structures from any shrapnel. These estimates were primarily based on the accident events discussed above.

3.2.6 Inert Vapor Cloud (LN2)

Since the ISO tank was filled with LN2, safety considerations associated with an inert gas cloud were considered to ensure safety of personnel on site.

3.2.7 Fire Source Thermal Radiation

The fire source was a high heat release rate pool fire type exposure and imposed a radiant heat flux to the surrounding environment. The estimated power of the exposure fire was used to calculate the expected incident heat flux to the surroundings.

---

[5] Hyde, D. W. (1988). User's Guide for Microcomputer Programs ConWep and FunPro, Applications of TM 5-855-1," Fundamentals of Protective Design for Conventional Weapons". US Army Engineer Waterways Experiment Station.

Literature correlations can be used to estimate various fire source characteristics.[6] Based on a fire area of 420 ft^2 (42 × 10 ft.), a 7,700-gallon liquid propane fire is estimated to produce a heat release rate of 178 MW, with an approximate flame height of 20 m, and burning duration of 73 minutes. Figure 4 shows input and output data for this calculation.

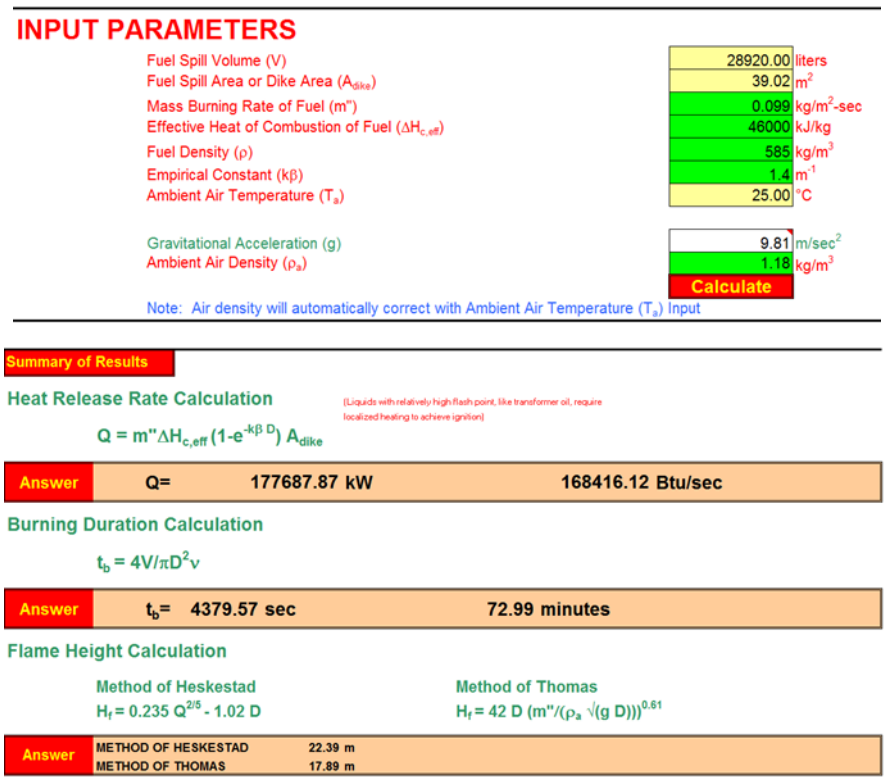

Figure 4. Calculated Fire Source Parameters for Liquid Propane Fire

Similar correlations can be utilized to estimate the incident heat flux to a target.[7] Based on the fire described above, the fire source was expected to provide an incident heat flux of approximately 1.5 kW/m^2 to the nearest tree line and less than 0.5 kW/m^2 at the closest structure. Figure 5 shows the input and output data for this calculation.

[6] NUREG 1805, FDT 3: 03_HRR_Flame_Height_Burning_Duration_Calculations_Sup1_SI.xls
[7] NUREG 1805, FDT 5: 05.1_Heat_Flux_Calculations_Wind_Free_Sup1_SI.xls

INPUT PARAMETERS

Mass Burning Rate of Fuel (m")	0.099	kg/m^2-sec
Effective Heat of Combustion of Fuel ($\Delta H_{c,eff}$)	46000	kJ/kg
Empirical Constant ($k\beta$)	1.4	m^{-1}
Heat Release Rate (Q)	177687.87	kW
Fuel Area or Dike Area (A_{dike})	39.02	m^2
Distance between Fire and Target (L)	61.00	m
Radiative Fraction (χ_r)	0.40	

OPTIONAL CALCULATION FOR GIVEN HEAT RELEASE RATE

Select "User Specified Value" from Fuel Type Menu and Enter Your HRR here → kW

Calculate

RADIATIVE HEAT FLUX CALCULATION

$q'' = Q \chi_r / 4 \pi R^2$

Answer	q" =	1.36 kW/m^2	0.12 Btu/ft^2-sec

Figure 5. Calculated Incident Heat Flux to Target

3.3 Preliminary Computational Fluid Dynamics (CFD)/Finite Element (FE) Modeling Calculations

FE analysis was used to support the development of the safety plan. The objectives of the modeling efforts included validating the model against known burst pressure performance data and to assess the temperature versus pressure time histories due to representative pool fire heat transfer rates. A quarter-scale model of a 12,164-gallon insulated LNG, based on a currently available and in-service product, was generated for use in the LS-DYNA (i.e., developed by the Livermore Software Technology Corporation [LSTC] in Livermore, CA) solver environment. See Figure 6 for a rendering of this quarter-scale model.

Figure 6. Quarter-Scale FE Model of Tank

The FE model consisted of eight parts representing the actual tank. These included the outer and inner walls, a multilayer insulation between the inner and outer walls, pipe connections between the walls, cylindrical supports, ring supports, LNG, and an air cavity. The model was meshed with 882,636 nodes, 766,800 solid (hexagonal) elements, and 58,800 shell (thick) elements. The use of thick shell elements versus standard 4-node shells facilitated surface temperature assignment to the model.

The model was validated against known pressure and temperature data for long-term thermal response under ambient conditions. The model was subjected to ambient temperatures in an implicit heat transfer simulation which represented a 53-day experiment. The initial temperatures of each part corresponded to temperatures representative of those that would exist in a normal operating environment and are depicted in Figure 7. A convective heat transfer boundary condition was prescribed to the exterior surface of the outer tank. The ambient temperature was specified using a temperature time history curve which incorporated cyclic variations in temperature based on the time of day as shown in Figure 8. Two simulations were conducted with different thermal properties specified for the insulation. The thermal conductivity value of the insulation was set to either an ideal or realistic value, which corresponds to a range of values from the literature.

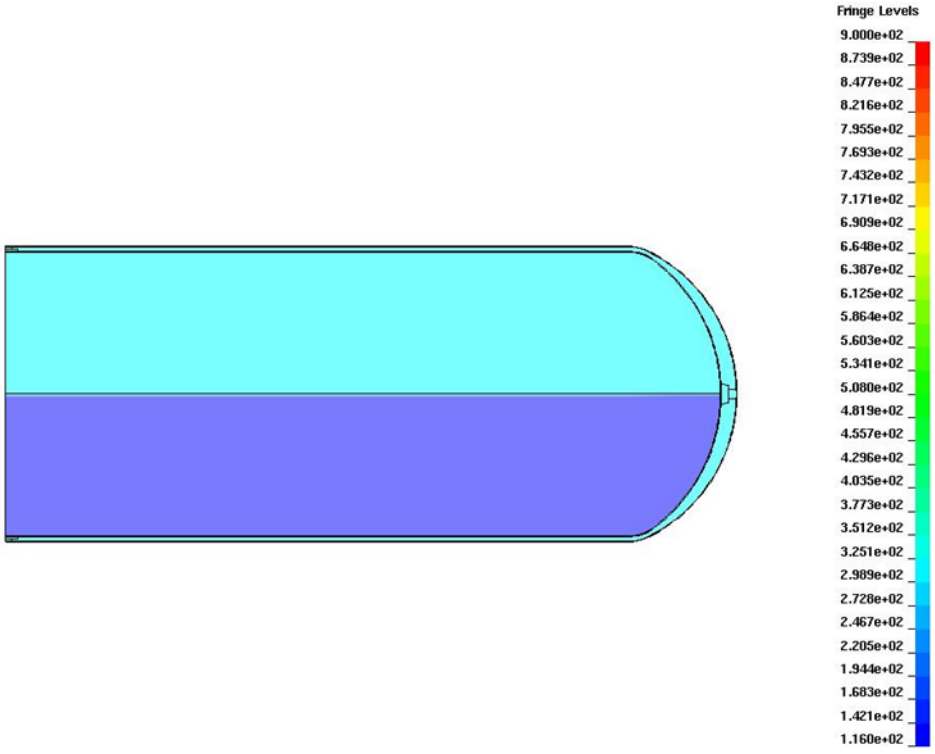

Figure 7. Fringe Diagram of Initialized Tank Part Temperatures; Relatively Cooler Temperatures Depicted by Colors Toward the Violet End of the Color Spectrum

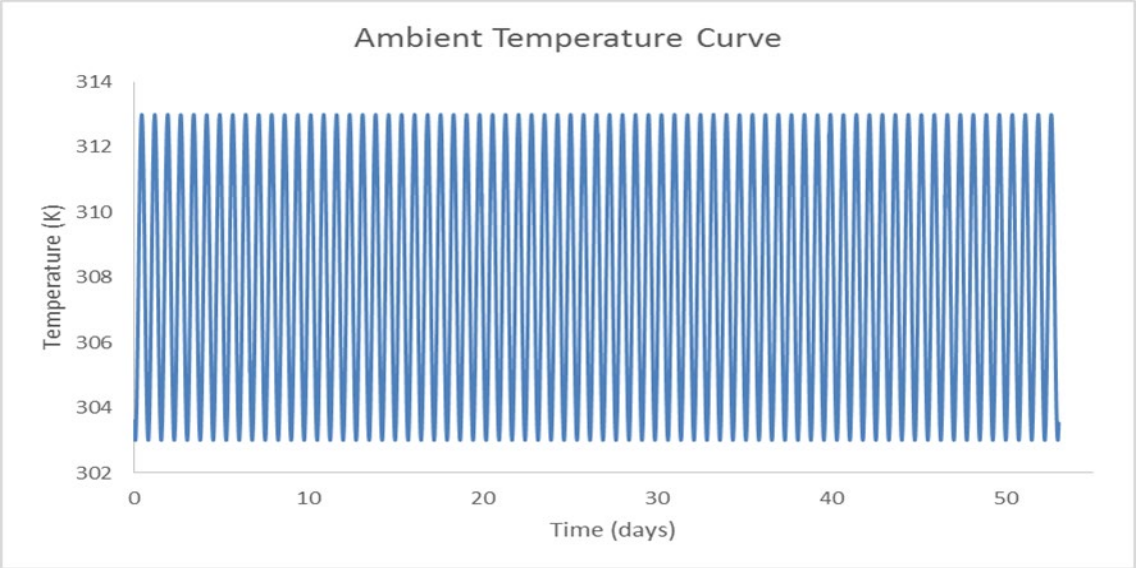

Figure 8. Ambient External Temperature (vertical axis) vs. Time for 53-day Test Simulation

The temperature and pressure time histories for tanks with insulation between the inner and outer tanks are provided in Figure 9. There are obviously large differences between the models with different insulation properties. This highlights the need to accurately characterize these properties for future work.

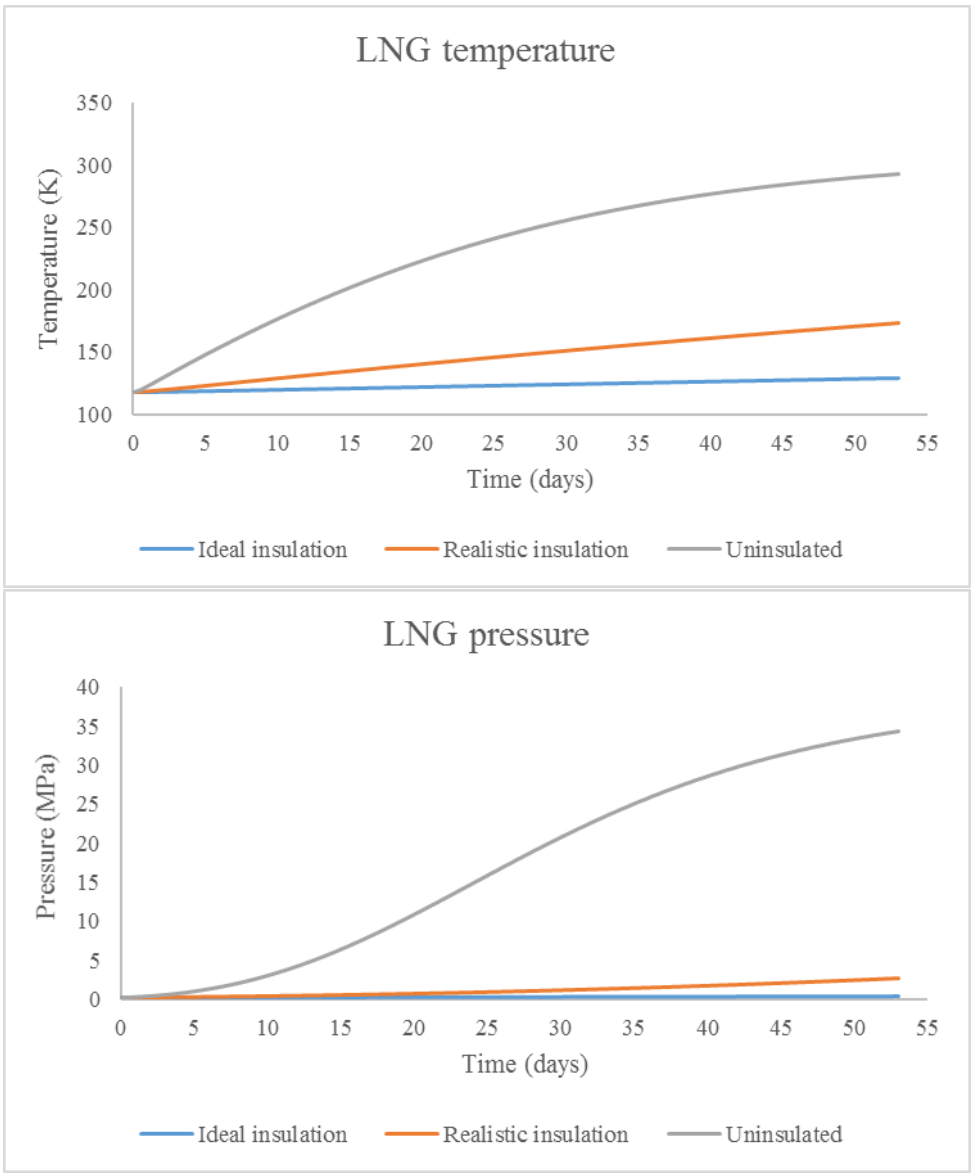

Figure 9. LNG Temperature (top) and Pressure (bottom) Time Histories for Three Simulations

4. Characterization of Fire Exposure Source

It was agreed between SwRI and FRA to consider a real accident scenario to determine the test duration. The following sections provide more detail about the assumed scenario, the calculated burning duration of the scenario (with the safety factor) and the fire source to be used in the experiment for this duration.

4.1 Accident Scenario

The accident scenario considered was a central ISO tank exposed to a 18.3 × 6.1-meter (60 × 20 ft.) LNG spill/fire by two adjacent ISO tanks. Each ISO tank has a capacity of approximately 37,854 liters (10,000 gal.) of LNG. Therefore, the time was calculated for 75,708 liters (20,000 gal.) of LNG to evaporate (over a 20-s spill time) and burn (over the remainder of the calculated duration), based on literature values of published regression rates. This time was then used to calculate the required amount of liquid propane needed to provide this test exposure.

4.2 Burning Duration Calculations

FRA provided a summary reference[8] on the topic of LNG regression rates in a series of large-scale experiments and recommended the rate to be used in this calculation.

An Excel workbook[9] was previously sent to FRA on December 21, 2016, which details the specific calculations and summarizes the input parameters used along with the relevant references for each input parameter. In addition, based on FRA input at the kickoff meeting, a safety factor of 2 was applied to the estimate. The conclusion of these calculations was that the test duration should be approximately 73 minutes. The amount of propane required was calculated based on an exposure area of 12.2 × 3.1 meters (40 × 10 ft.) (nominal footprint of ISO tank on flatcar) and for a test duration of 73 minutes.

A sheet was added to the burning duration workbook,[10] which estimates the required amount of propane to achieve the 73-minute burning duration. These estimates are based on literature burning rates for propane.[11] Based on these calculations, the required amount of propane for this experiment was approximately 30,283 liters (8,000 gal.).

4.3 Fire Source

A propane burner system was designed to simulate a pool fire for exposure of the LNG tank. The Freidman Research Corporation (FRC) supported the design and implementation of the burner system with CFD analysis and small-scale testing. SwRI provided FRC with the required capacity and prototypical design of the system. The requirements were as follows:

- Burner footprint: 12.2 × 3.1 meters (40 × 10 ft.)

[8] Raj, P., "LNG fires: A review of experimental results, models and hazard prediction challenges," Journal of Hazardous Materials 140 (2007) 444–464, doi:10.1016/j.jhazmat.2006.10.029.
[9] Huczek, J., "Burning Duration Estimates.xlsx," email correspondence to Federal Rail Administration, December 2016.
[10] Ibid.
[11] Hurley, M., et al., "SFPE Handbook of Fire Protection Engineering, 5th Edition, Chapter 26: Heat Release Rates," pp. 863–867, doi: 10.1007/978-1-4939-2565-0_26, Society of Fire Protection Engineers, 2016.

- Fuel: LPG
- Capacity: 378.5 liters/minute (100 gpm) of LPG

The initial concept for the burner design is shown schematically in Figure 10 and includes eight 2.4-meter (8-ft.) long branches extending between two 12.2-meter (40-ft.) manifolds. Each branch was to be pre-drilled with a number of holes of a determined size to allow liquid propane to flow through. The initial design called for the burner assembly to be submerged in approximately 0.1 meter (4 in.) of water which would serve to diffuse the flowing propane and protect the assembly from the heat of the fire. The objectives of the work performed by FRC were to determine the appropriate size and quantity of holes in each branch and identify any unforeseen issues related to the performance of the system.

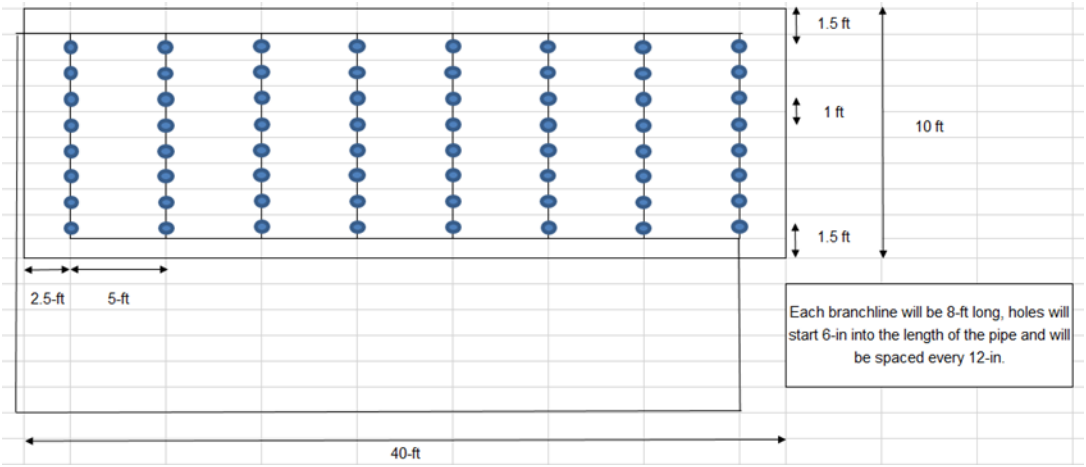

Figure 10. Preliminary Burner Design Concept

The performance of the burner design was evaluated using three different approaches. These two CFD solvers, Pipe Flow Expert (i.e., Daxesoft Ltd. in Cheshire, England) and EXN/Aero (i.e., Envenio in Fredericton, NB, Canada), were used to evaluate the performance of the system both at the scale of the individual holes and for the full system. Small-scale physical testing was used to evaluate the effects of hole sizes on liquid propane flow and vaporization as well as to investigate unknown outcomes related to the test conditions. A Fire Dynamics Simulator (FDS) (i.e., National Institute of Science and Technology [NIST] in Gaithersburg, MD, and Valtion Teknillinen Tutkimuskeskus [VTT], Technical Research Centre of Finland) was used to evaluate the effect of the pool fire and environmental characteristics on heating the LNG tank.

4.3.1 Fluid Dynamics

A small-scale CFD simulation of a single burner branch (8-ft. long, 8 holes) was developed to identify the K-factor for liquefied petroleum gas flowing through an orifice, Figure 11. The results predicted a K-factor of 0.96. A full-scale burner design was modeled using Pipe Flow Expert, as shown in Figure 12, using the K-factor value identified in the small-scale CFD work. The model included a differential pump, 32-meter (105-ft.) pipe from pump to manifolds, 2 × 19.1-meter (40-ft.) branch lines, the burner assembly, as well as all pipe connections. The number and size of outlets was varied as was the total LPG flow rate, and vertical elevations of various regions of the pipe.

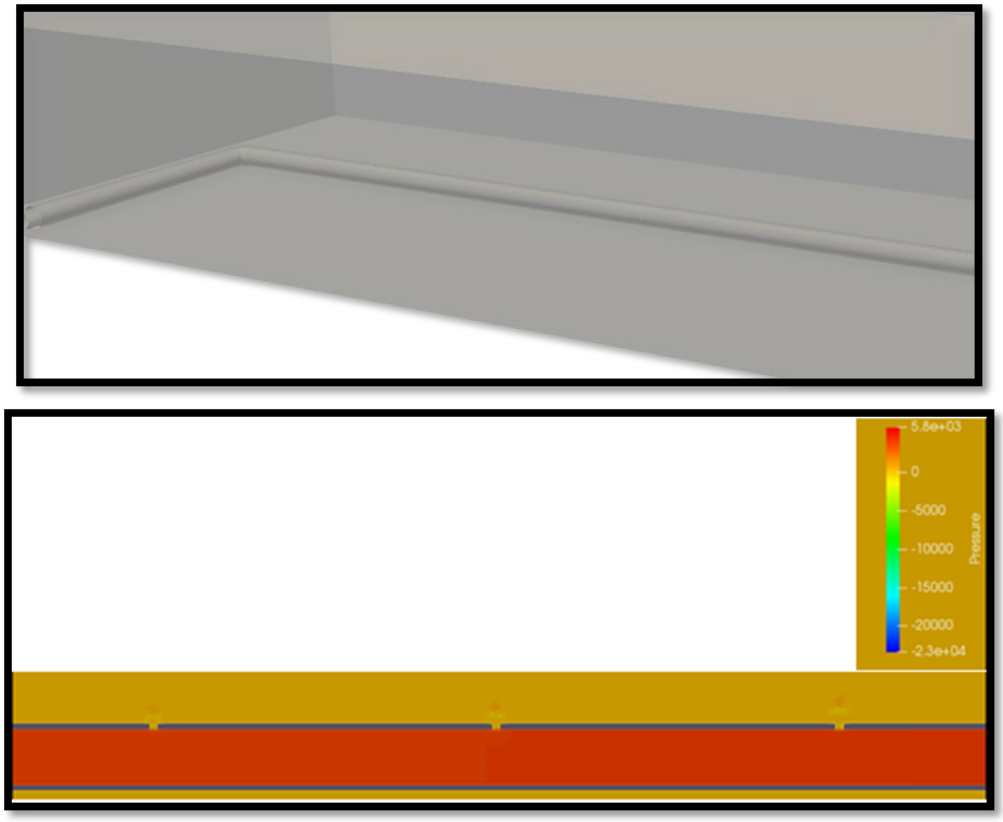

Figure 11. CFD Model of Single Burner Branch (top) and Cross-section Fringe Plot of Pressure (bottom)

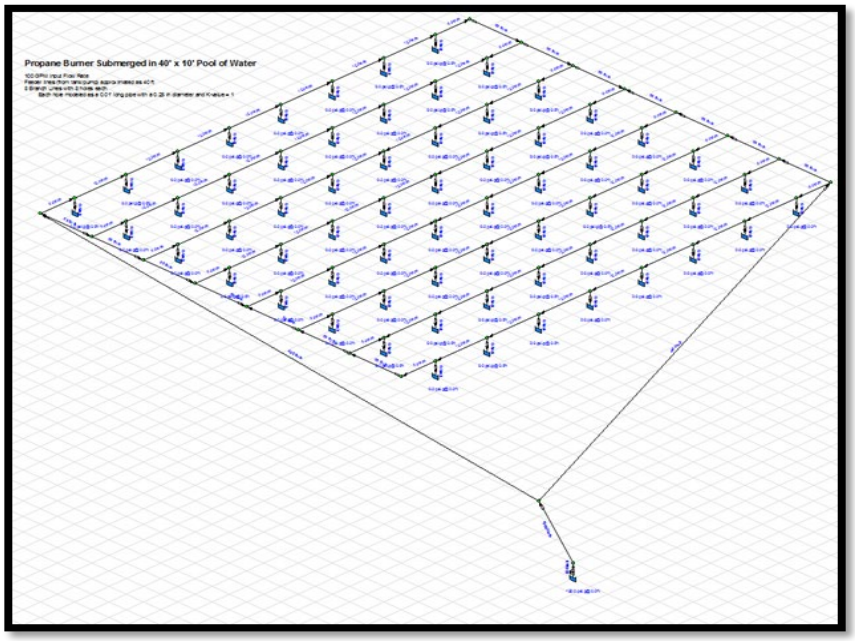

Figure 12. Full Scale Burner Model Implemented in Pipe Flow Expert

Nearly equal flow (1.565 ± 0.005 gpm per 1/8-in. hole; 1.58 ± 0.03 gpm per 1/4-in. hole) was calculated for each of the 64 × 1/8-in. holes at a total flow rate of 100 gpm. The flow rate out of each hole continued to be very evenly distributed across all 64, 96, or 128 orifices independent of orifice size (1/8 in. or 1/4 in.). High exit velocities were calculated for a vertical elevation difference of 4-in. between the end branches of the burner matrix resulted in about a 10 percent difference in flow rate out of each branch. Note that the program is unable to account for vaporization of a liquid, however, the calculated pressures within the entire burner matrix remained above vaporization pressure. A differential pump with speed control could suitably alter the total flow rate from 50 gpm to 100 gpm with no negative effects on the performance of the system; even flow rate out of all orifices was maintained at the lower flow rates.

4.3.2 Small Scale Testing

A small-scale test was set up to investigate the effects of flowing LPG through a representative burner system and to identify unforeseen issues with this burner design. Liquid propane flowed through variations of small-scale burner assemblies that consisted of 12-inch to 36-inch lengths of 1/2-inch, 1-inch and 2-inch diameter, schedule 40 black pipe. A 33-lb (8-gal.) "forklift cylinder" propane tank with a dip tube was used to supply the flow of liquid propane into the burner assembly via a 6-foot long hose. The burner assembly was made with several 1/16-inch, 1/8-inch, and 1/4-inch diameter holes as shown in Figure 13 and summarized in Table 1. The burner was submerged in under a depth 1 inch to 4 inches of water for each test. A digital scale (i.e., model No. SD35, Ohaus Corporation in the U.S.) was used to provide a time-history of the propane mass from which a flow rate could be calculated. Figure 14 depicts a typical test.

Figure 13. Small-Scale LPG Burner Test Setup

Table 1. Summary of Small-Scale Burner Tests

Hole Diameter (in.)	Number of Holes	Pipe Diameter (in.)	Vol. Flow Rate (gpm)	Spray Height (ft.)	Notes
0.0625	1	0.5	0.75	7	
0.125	1	0.5	0.75	5	
0.125	2	0.5	1.14	4	
0.25	1	0.5	0.9	3	ICE
0.125	1	1	0.25	5	
0.25	1	1	0.25	3	ICE
0.25	2	1	1.25	3	ICE
0.25	1	2	1	3	
0.25	2	2	1.5	3	ICE
0.125	3	2	1.5	4	

Figure 14. (3) × 1/8-in. Diameter Holes, 2-in. Diameter Pipe, 1.5 gpm

For each test, the pipe was initially submerged in and filled with water. As the flow of propane was initiated, the water was quickly expelled through the pre-drilled orifices. In all tests, the propane appeared to remain liquid until escaping through the orifices at which point it quickly changed phase and expanded rapidly. The rapid phase change and expansion into a gas had two negative effects. The interaction between the LPG and the water surrounding the orifices resulted in the formation of ice around the orifices under certain situations, which discussed below. Additionally, the rapid expansion of the LPG liquid as it vaporized into gas resulted in jets of LPG/water that reached as high as 5-feet and produced a large amount of spray. The height of the jets decreased with increasing orifice size. Two examples of jet height are shown in Figure 15.

Figure 15. Left: Height of Spray from Single 1/8-in. Hole (~4-5-ft. tall); Right: Height of Spray from Single 1/4-in. Hole (~3-ft. tall)

The most important effect related to hole size was the generation of ice on the orifice. The 1/4-in. diameter holes always produced ice at flow rates up to 1.25 gpm. Ice occasionally occurred at the 1/4-in. diameter orifices at 1.5 gpm. Ice formation was reduced with the use of smaller holes. Ice always formed at the hydraulically most remote hole first and then propagated toward the pressure source if the overall flow rate was not high enough to prevent ice buildup. When ice did form, it generally fully covered or significantly restricted the flow through an orifice within 30 seconds of initiating the flow. An example of the resulting flow after ice buildup is shown in Figure 16.

Figure 16. Ice Buildup: (2) × 1/4-in. Diameter Hole in 2-in. Diameter Pipe at 1.5 gpm

To reduce the height of the jets produced by the vaporization of the LPG three cover designs were implemented as shown in Figure 17. All the covers prevented jets from occurring, as shown in Figure 18, however, they also increased the generation of ice. A flat plate (2-in. wide) mounted 1.75 inches above the 3 × 1/8-inch diameter holes provided adequate dissipation of the jet while also limited ice formation; some amount of ice still formed, but did not appear to affect the flow rate out of the orifices.

Figure 17. Select Covering Methods to Reduce Spray; 2-in. Angle Iron, 2-in. Wide Plate, 1-in. Diameter PVC Tubing Split Lengthwise

Figure 18. (3) × 1/8-in. Diameter Holes in 2-in. Diameter Pipe with 2-in. Wide Plate Cover, 1-in. Gap Between Steel Plate and Pipe Holes, 1.5 gpm

4.3.3 Fire Dynamics Simulator (FDS) Pool Fire Evaluation

FDS was used to evaluate the effect of the pool fire and environmental characteristics on heating the LNG tank. A full-scale tank supported on a flatcar was modeled which included only the outside surfaces of the components, shown in Figure 19. The pool fire was modeled with an area of 400 ft^2 with propane as a reactant and the heat release rate specified directly using a heat release rate per unit area (HRRPUA). The height of the flames, wall temperature of the tank (max and mean), and the density of the reactants were evaluated. The HRRPUA and wind speed (directed along the longitudinal axis of the tank) were varied to determine their effects of tank heating. The HRRPUA values that were evaluated are specified in Table 2.

The simulations were not validated against test data, and were not assumed to provide a high level of accuracy regarding specific temperature measurements. However, the FDS modelling work was intended to provide representative gross characteristics of the pool fire and the general large-scale effects of select input variables such as HRRPUA and Wind. Thus, most simulations were conducted for a time period selected to ensure that the model was able to stabilize—generally, 100–200 seconds.

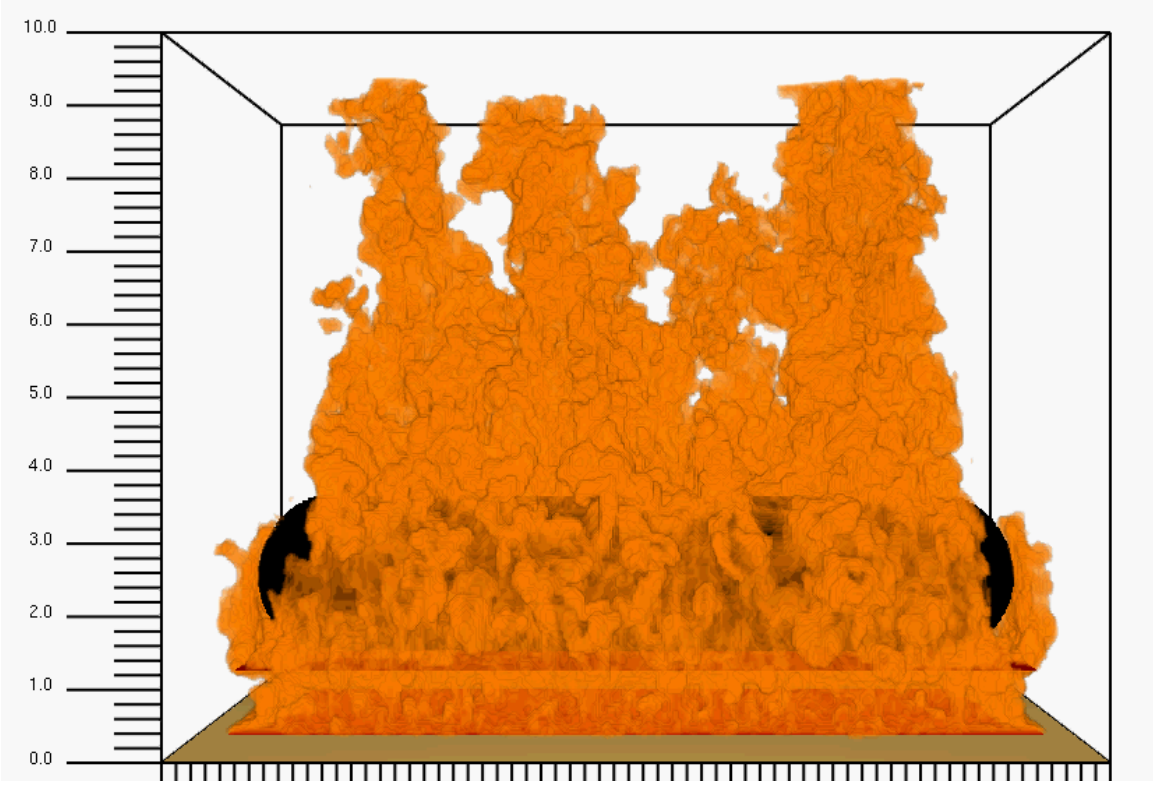

Figure 19. FDS Model of Tank and Flatcar

Table 2. HRRPUA Values Applied for FDS Analysis

Simulation	HRRPUA (kW/m^2)	Wind speed (mph)
Full	4,564	0
Three-quarter	3,423	0
Half	2,282	0
Wind – Full	4,564	5
Wind - Half	2,282	5

The flame heights calculated in each simulation with select HRRPUA values (i.e., Full, Three-Quarter, Half) are shown in Figure 20. It was clear that the greater HRRPUA values resulted in greater flame volume and overall height. The peak outer tank wall temperature varied by approximately 50 ºC between the Full and Half HRRPUA models, as shown in Figure 21. Much smaller variations were calculated for average tank temperature (Figure 22). A notable observation regarding the test setup is that the railcar appeared to deflect a significant amount of heat away from the tank. The effect of a 5-mph wind was significant (see Figure 23 and Figure 24), especially for the Half HRRPUA simulation in which the peak temperature was reduced by

over 100 ºC. The average outer tank wall temperature was more sensitive to wind and fuel rate than peak temperatures.

Finally, the ability to fully combust the amount of propane required to produce the desired HRRPUA was evaluated. A maximum HRRPUA of 4,564 kW/m^2 was identified by SwRI as approximately equivalent to the LPG exposure fire planned for testing. The density of propane reactants for the Full and Half HRRPUA simulations was calculated at two heights: 1.5-feet and 11.5 feet above the ground to determine how much propane was combusted. Note that the combustion parameters were defined to simulate ideal conditions. As depicted in Figure 25, 97–99 percent of all propane was able to be combusted by the time it reached 11.5 feet. On the other hand, about 25 percent and 50 percent of the propane in the Full and Half HRRPUA simulations, respectively, had yet to combust at 1.5 feet above the ground.

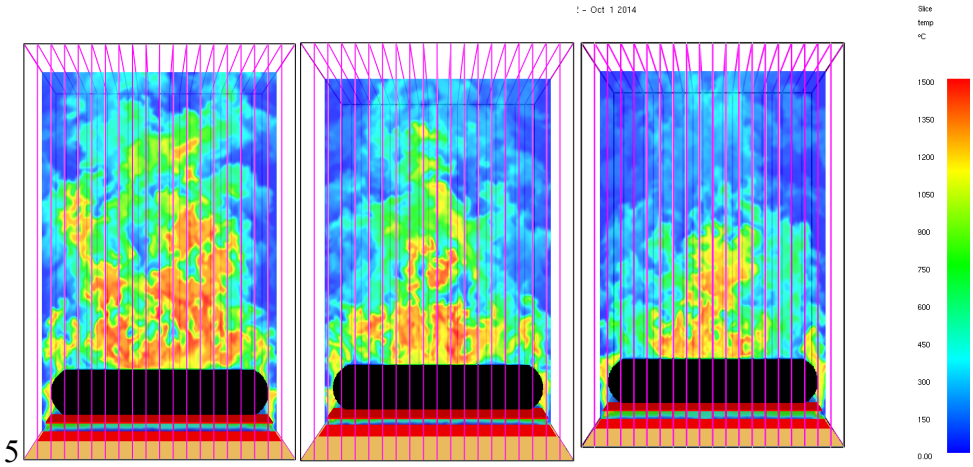

Figure 20. Flame Height Comparison for Full, Three-quarter, and Half HRRPUA FDS Simulations, NB: Total Mesh Height Is 20 m

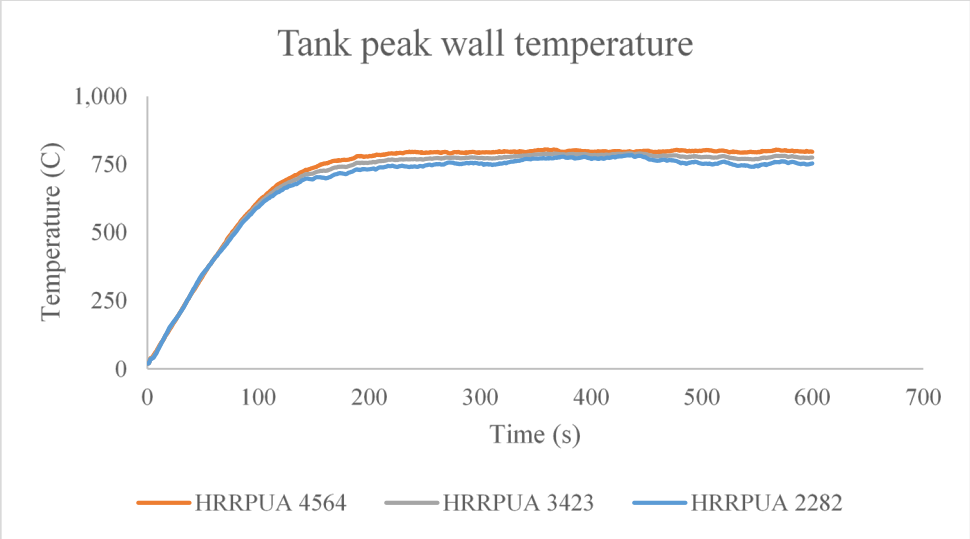

Figure 21. Maximum Outer Wall Temperature of the Tank by HRRPUA

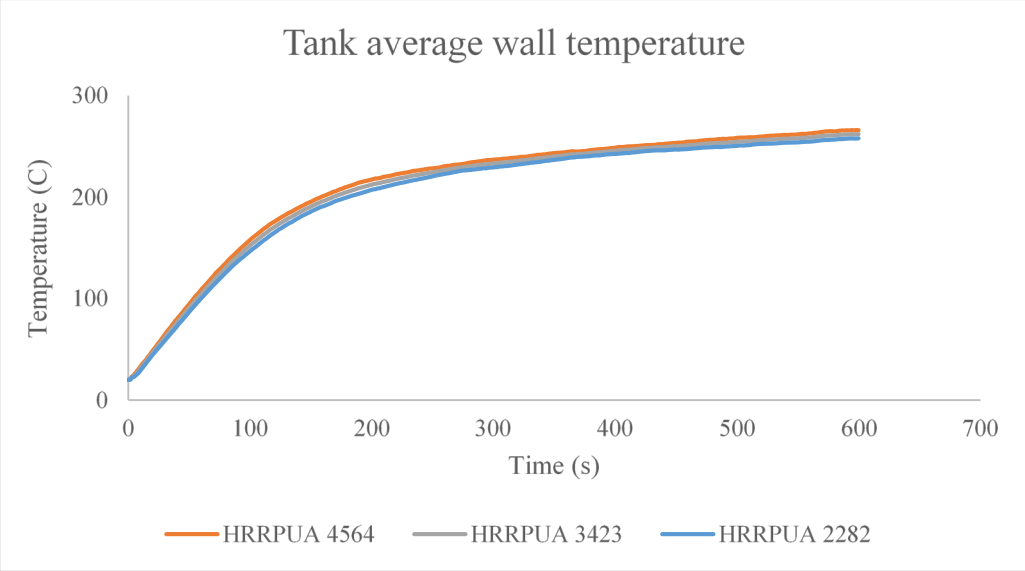

Figure 22. Mean Outer Wall Temperature of the Tank by HRRPUA

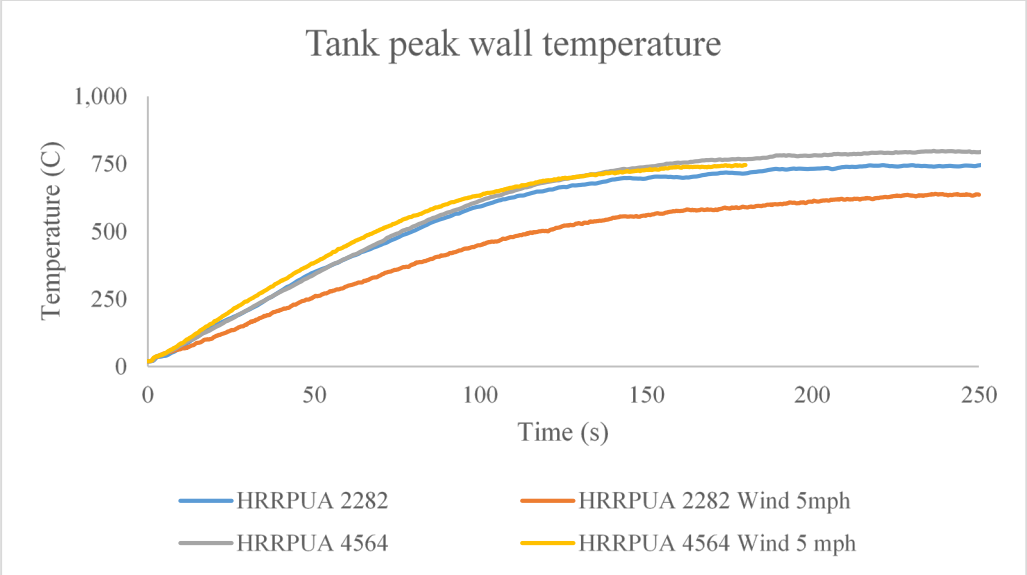

Figure 23. Effect of 5-mph Wind on Peak Outer Wall Tank Temperature

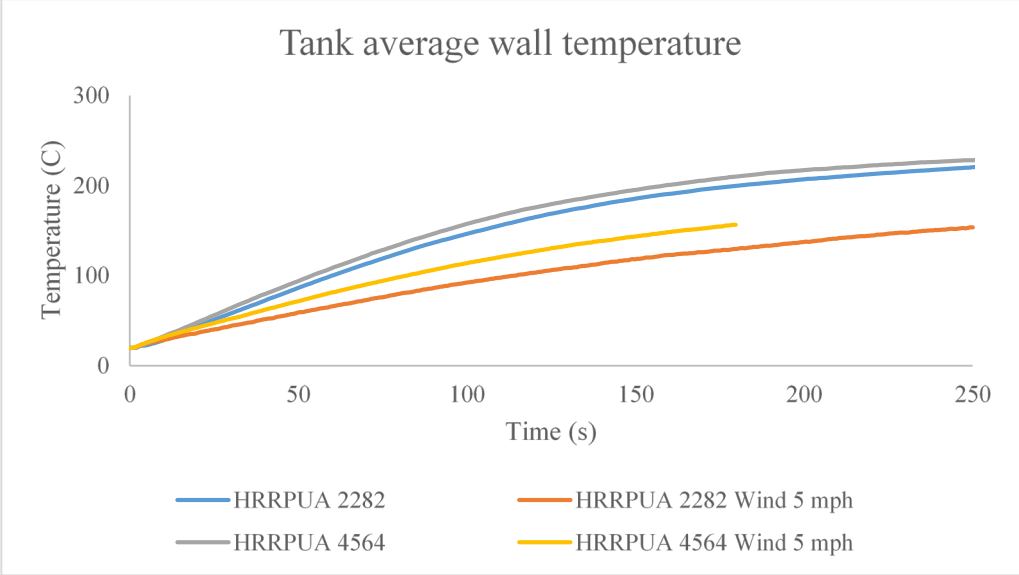

Figure 24. Effect of 5-mph Wind on Average Outer Wall Tank Temperature

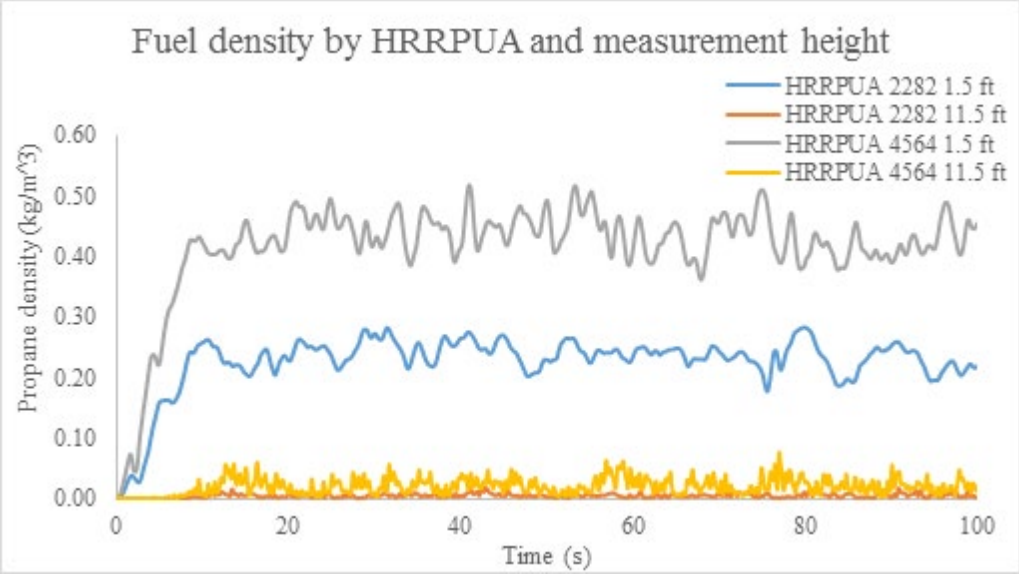

Figure 25. Fuel Density by HRRPUA and Measurement Height

4.3.4 Final Fire Source Recommendations

The CFD analysis and small-scale testing provided valuable information about the burner assembly design. The suggested design parameters are listed below:

- Limit vertical elevation differences of burner assembly to less than 4 inches to maintain even flow (< 10 percent difference) through all orifices
- Use 1/8-inch diameter orifices to prevent ice buildup
- Increase the depth of water submersion or invert the burner assembly to reduce the amount of spray

4.4 Final Fire Source Conditions

The fire source consisted of a 40 × 10-foot (nominal footprint of ISO tank on flatcar) LPG burner. A piping array was installed in the steel burner pan. The array had 8 branch lines and each branch line had 24 1/8-inch diameter holes. The piping array was installed in the burner pan with the holes pointed downward, which allowed the LPG to diffuse more evenly through the water layer contained in the burner pan. LPG was fed to the burner array at the northeast and southwest corners from a 2-in. buried pipe. An LPG supply system consisting of an 8,000-gallon LPG tank, pump loop, and flow meter was set up approximately 850 feet away from the test area. An emergency stop button was routed to the adjacent control room to allow test personnel to safely stop the flow of LPG to the burner, in case of an emergency.

5. Test Instrumentation

Several types of instrumentation were utilized in this experiment. A total of 18 internal temperature measurements were taken, in addition to internal tank pressure, annular space vacuum pressure (between the inner and outer tanks), and PRD line pressure. Externally, nine thermocouples (TCs) were provided around the tank and fire source to characterize the convective heat transfer rate from the fire and measure boundary layer temperatures.

An additional 18 TCs were used to characterize the total heat flux from the fire and into the tank at several locations. Incident heat flux was measured at two ground-based (3 ft. above grade) targets. Instruments were also provided at some distances from the tank to measure blast pressures, if any, resulting from catastrophic tank failure. Finally, the liquid propane flow rate and the wind speed were measured (wind direction sensor was not operating correctly, but wind direction was out of the east at the beginning of the test, and slowly moved more north during the test, based on windsock observations). The test was also documented with HD cameras from three views.

Two data acquisition systems (DAQs) were utilized. One ("high-speed DAQ") was used to collect the thermal instrumentation and pressures (1 Hz) as well as the blast pressure data (10 kHz). The other ("slow-speed DAQ") was used to collect the propane flow rate and wind speed (1 Hz).

Table 3 and Table 4 provide lists of the instrumentation and channel assignments utilized for the high-speed DAQ and slow-speed DAQ, respectively. Additional details are provided in the subsequent sections.

Table 3. High-Speed DAQ Test Instrumentation List

Channel No.	Description*	DAQ ID
1	Non-piping End baffle – top gas/liquid temperature	NPE-#1
2	Non-piping End baffle – middle gas/liquid temperature	NPE-#2
3	Non-piping End baffle – right side surface temperature	NPE-#3
4	Non-piping End baffle – left side surface temperature	NPE-#4
5**	Non-piping End baffle – bottom gas/liquid temperature	NPE-#5
6**	Non-piping End baffle – bottom surface temperature	NPE-#6
7	Center baffle – top gas/liquid temperature	C-#1
8	Center baffle – middle gas/liquid temperature	C-#2
9	Center baffle – right side surface temperature	C-#3
10	Center baffle – bottom gas/liquid temperature	C-#4
11	Center baffle – left side surface temperature	C-#5
12	Center baffle – bottom surface temperature	C-#6
13	Piping end baffle – top gas/liquid temperature	PE-#1
14	Piping end baffle – middle gas/liquid temperature	PE-#2
15	Piping end baffle – bottom gas/liquid temperature	PE-#3
16	Piping end baffle – bottom surface temperature	PE-#4
17	Piping end baffle – left side surface temperature	PE-#5

Channel No.	Description*	DAQ ID
18	Piping end baffle – right side surface temperature	PE-#6
19	Non-piping end baffle – right side weld-pad external surface	NPE-#3-EXT
20	Center baffle – right side weld-pad external surface temperature	C-#3-EXT
21	Piping end baffle – right side weld-pad external surface	PE-#6-EXT
23	Non-piping end baffle – east side differential flame thermometer	NPE-E-DFT-B
24	Center baffle – east side differential flame thermometer – front	C-E-DFT-F
25	Center baffle – east side differential flame thermometer – back	C-E-DFT-B
27	Piping end baffle – east side differential flame thermometer –	PE-E-DFT-F
28	Piping end baffle – east side differential flame thermometer –	PE-E-DFT-B
29	Non-piping end baffle – east side differential flame thermometer	NPE-E-DFT-F
32	Non-piping end baffle – left side weld-pad external surface	NPE-#4-EXT
33	Center baffle - left side weld-pad external surface temperature	C-#5-EXT
34	Piping end baffle – left side weld-pad external surface	PE-#5-EXT
35	Non-piping end baffle – West side differential flame	NPE-W-DFT-
36	Non-piping end baffle – West side differential flame	NPE-W-DFT-
37	Center baffle – west side differential flame thermometer – front	C-W-DFT-F
38	Center baffle – west side differential flame thermometer – back	C-W-DFT-B
39	Piping end baffle – west side differential flame thermometer –	PE-W-DFT-F
40	Piping end baffle – west side differential flame thermometer –	PE-W-DFT-B
41	Non-piping end baffle – fire source differential flame	NPE-FS-DFT-
42	Non-piping end baffle – fire source differential flame	NPE-FS-DFT-
43	Non-piping end baffle – fire source gas temperature	NPE-FS-GT
44	Center baffle – fire source differential flame thermometer –	C-FS-DFT-B
45	Center baffle – fire source differential flame thermometer –	C-FS-DFT-F
46	Center baffle – fire source gas temperature	C-FS-GT
47	Piping end baffle – fire source differential flame thermometer –	PE-FS-DFT-B
48	Piping end baffle – fire source differential flame thermometer –	PE-FS-DFT-F
49	Piping end baffle – fire source gas temperature	PE-FS-GT
50	Copper disc for incident heat flux – north – front	CD-N-F
51	Copper disc for incident heat flux – north – back	CD-N-B
52	Copper disc for incident heat flux – west – front	CD-W-F
53	Copper disc for incident heat flux – west – back	CD-W-B
54	Internal tank pressure	IT-P
55	Annular space tank pressure	AST-P
56	Pressure relief valve discharge pressure	PRV-P
BNC1	Blast pressure probe – north	BP-N
BNC2	Blast pressure probe – west	BP-W

*Non-fire source DFTs – Back = Tank Side; Front = Fire Side; Fire Source DFTs – Back = Tank Side; Front = Fire Side; Copper Discs – Front = Exposed Copper Disc, Back = Internal TC.

** Channels 5 and 6 Type T TCs not responding at beginning of test.

Note: Skipped channels 22, 26, 30, 31, and 57–60.

Table 4. Slow-Speed DAQ Test Instrumentation List

Channel No.	Description	DAQ ID
1	Liquid propane flow rate	LPG-GPM
2	Wind speed	WS-MPH
3	Wind direction (not operational during experiment)	WD-DEG

5.1 Internal Instrumentation

Internal instrumentation included the gas/liquid temperatures measured inside the test tank, as well as the internal tank pressure, the annular space tank pressure and the pressure relief discharge pressure. SwRI worked with CVA and one of their vendors, Conax Technologies, LLC, to accommodate internal temperature measurements. Figure 26 and Figure 27 were provided by CVA and show the installed arrangement of thermocouple trees as well as the location of the external weld-pad thermocouples, as installed by CVA during fabrication of the tank. Figure 28 provides layout drawing for the pass-through connectors utilized for the internal temperature sensors. These figures are also provided in Appendix B.

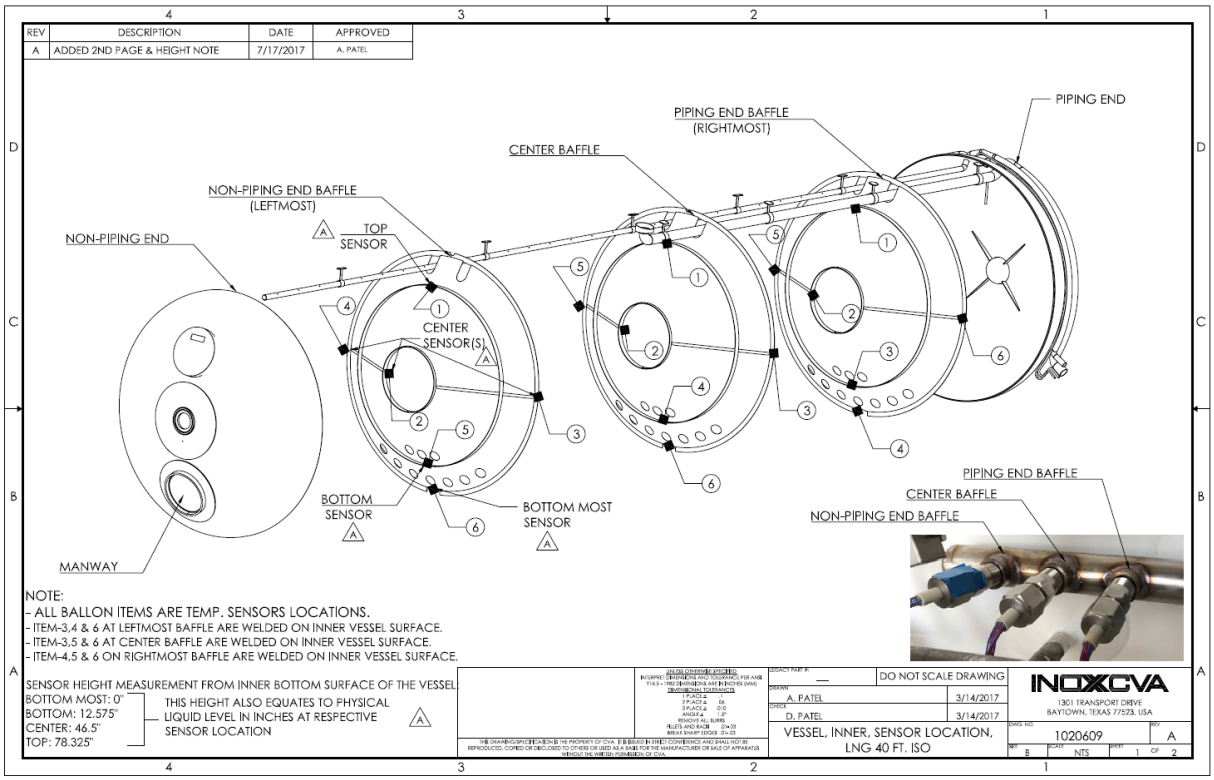

Figure 26. Arrangement of Thermocouple Trees in Inner Tank (provided by CVA)

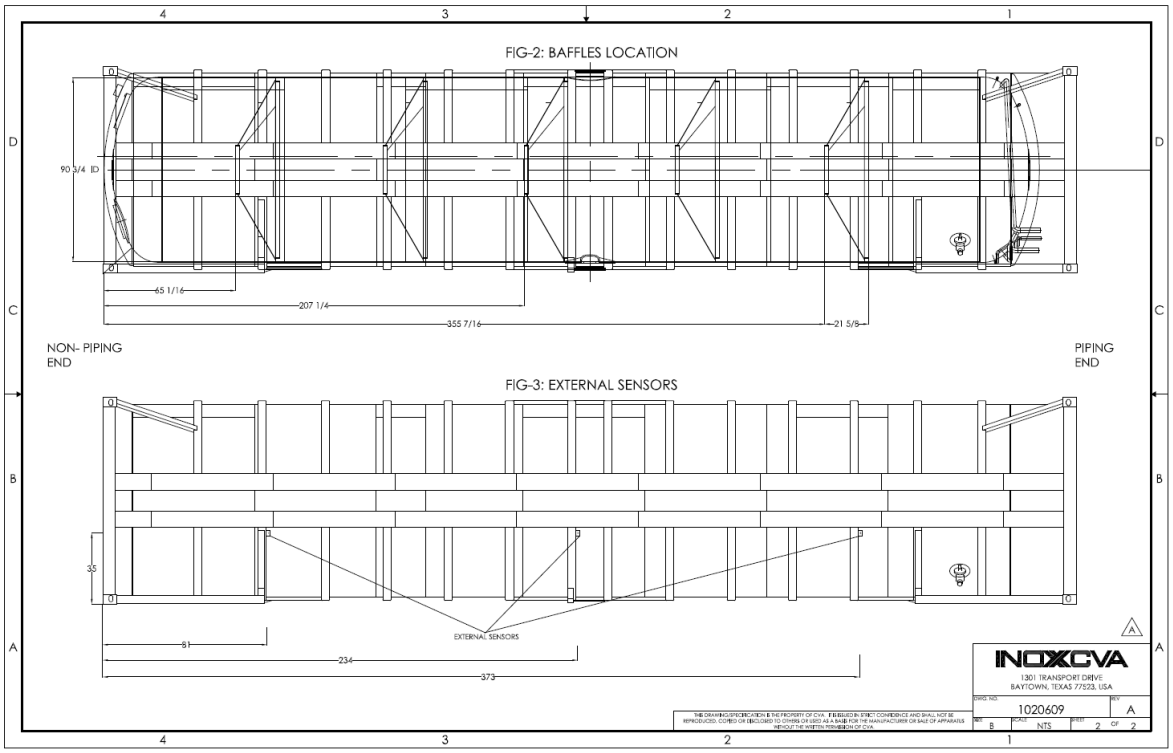

Figure 27. ISO Tank Showing Location of Baffles in Plain View and External Weld-Pad Thermocouples in Elevation View (provided by CVA)

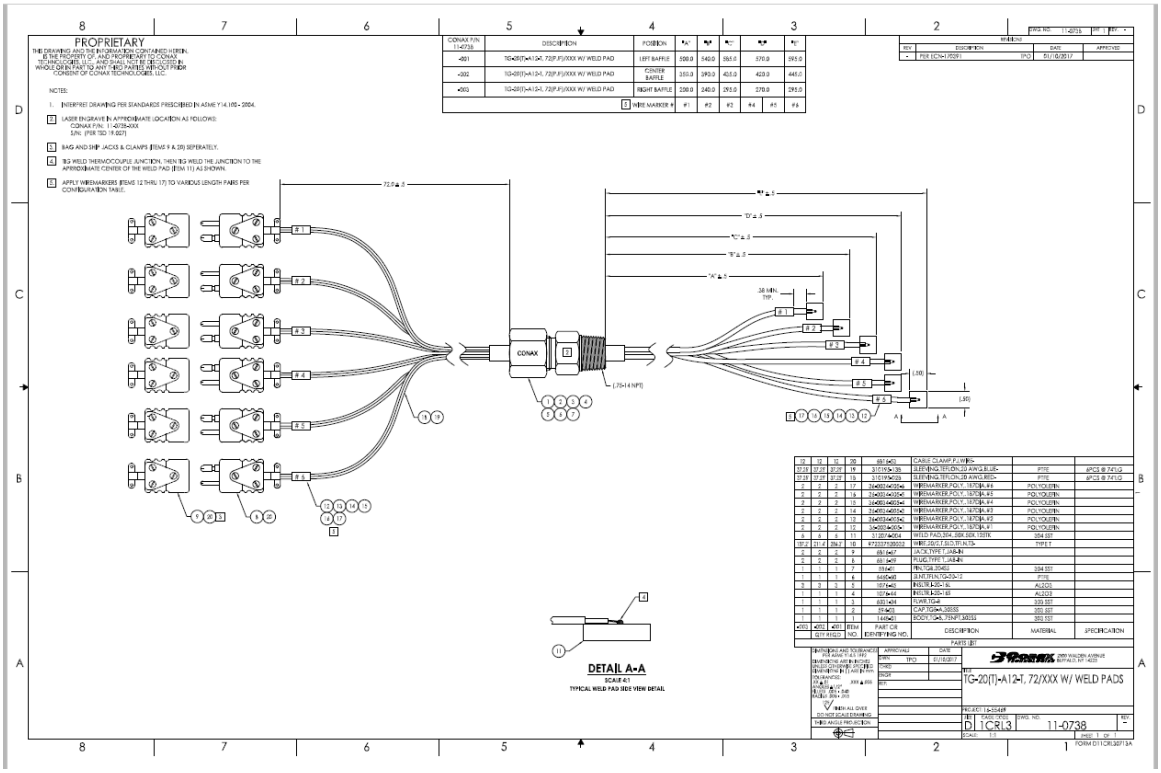

Figure 28. Internal Temperature Pass-Through Connector Drawing

5.2 External Instrumentation

The external instrumentation included TCs used to characterize the fire source intensity, the heat flux at the exterior of the test tank, and incident heat flux downrange to targets.

In addition to the thermal instrumentation described above, video and photographs have been archived and delivered to FRA for their review. A selected group of photographs are included in this report.

5.2.1 Directional Flame Thermometer (DFT)

The directional flame thermometer (DFT) was originally developed for measuring temperatures and heat fluxes in pool fires.[12] The DFT is conceptually similar to the plate thermometer but consists of two 3-mm thick, 120 × 120-mm Inconel plates with a 25-mm thick ceramic fiber blanket in between (see Figure 29). The blanket is compressed to 19-mm thickness. A 1.6-mm diameter sheathed type K TC with an insulated junction is located in a groove on the inside of each plate.

[12] Keltner, N., Nash, L., Beitel, J., Parker, A., Welsh, S., and Gilda, B., (2001). "Fire Safety Test Furnace Characterization Unit," ASTM STP 1427, Thermal Measurements: The Foundation of Fire Standards, Dallas, TX, 128–146.

An advantage of the DFT over the plate thermometer is that the heat transfer through a DFT can be calculated with an inverse heat transfer code such as IHCP1D.[13] The use of these devices in fire experiments has been recently standardized in ASTM E3057.[14]

Figure 29. Directional Flame Thermometer

5.2.2 Weld-Pad Surface Temperature

The weld-pad surface temperature thermocouple probe is designed for use in industrial applications to measure surface temperature by way of attachment via weld, braze, or clamp. The pad is flexible to easy form to the contour of a flat or curved surface. The pad material is 304 stainless steel and measures 1.0 × 1.0 × 0.01 inch (25 mm × 25 mm × 0.25 mm) and the thermocouple is type K. Figure 30 shows a photograph of one of SwRI's weld-pad thermocouples.

Figure 30. Weld-Pad Surface Temperature Thermocouple Probe

[13] Beck, J., (1999). "User's Manual for IHCP1D, a Program for Calculating Surface Heat Fluxes from Transient Temperatures Inside Solids," Beck Engineering Consultants Co., Okemos, MI.
[14] "ASTM E3057-16: Measuring Heat Flux Using Directional Flame Thermometers with Advanced Data Analysis Techniques." ASTM International, West Conshohocken, PA.

5.2.3 Copper Disc Calorimeter

Incident heat flux downrange were calculated from the response of a custom designed copper disk calorimeter. The sensor consists of a thin copper disc, approximately 0.3 mm (12 mil) in thickness and 13 mm (1/2 in.) in diameter. The chromel and alumel wires of a 24 AWG type K TC are silver-soldered to the back side of the disc. The TC wires are then pulled through small holes and taped to the backside of a 13-mm (1/2-in.) thick, 100 × 100 mm (4 × 4 in.) piece of ceramic fiber board (Unifrax Duraboard LD), so that the copper disc is in contact with the exposed surface of the ceramic fiberboard, as shown in Figure 31. The exposed side of the copper disc and ceramic fiberboard are coated with a thin layer of black, heat-resistant paint with a known emissivity/absorptivity of 0.9 (Thurmalox® Solar Collector Coating, 250 Selective Black).

The ceramic fiber board is backed by a 13-mm (1/2-in.) thick calcium silicate substrate, which is backed by a 25-mm (1-in.) think layer of ceramic fiber blanket. All of these materials are housed in a small metal enclosure measuring 100 × 100 × 50-mm deep (4 × 4 × 2-in. deep). The housing and additional substrates are not pictured below.

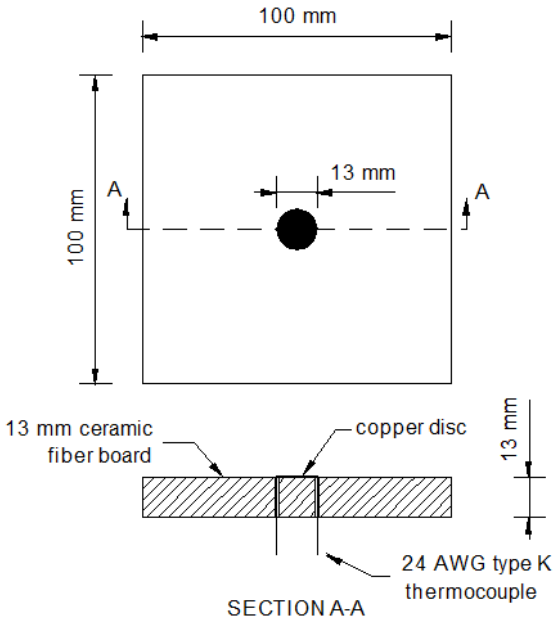

Figure 31. Copper Disc Calorimeter

5.2.4 General Instrumentation Layout Sketch

Figure 32 provides a plan view general layout of the external instrumentation at the remote site. Note that the fire source DFTs depicted in red are located between the fire source and underside of the flatcar. The DFTs depicted in green are touching the outer tank wall at the same nominal location as the weld-pad TCs and internal TCs at the same baffle position.

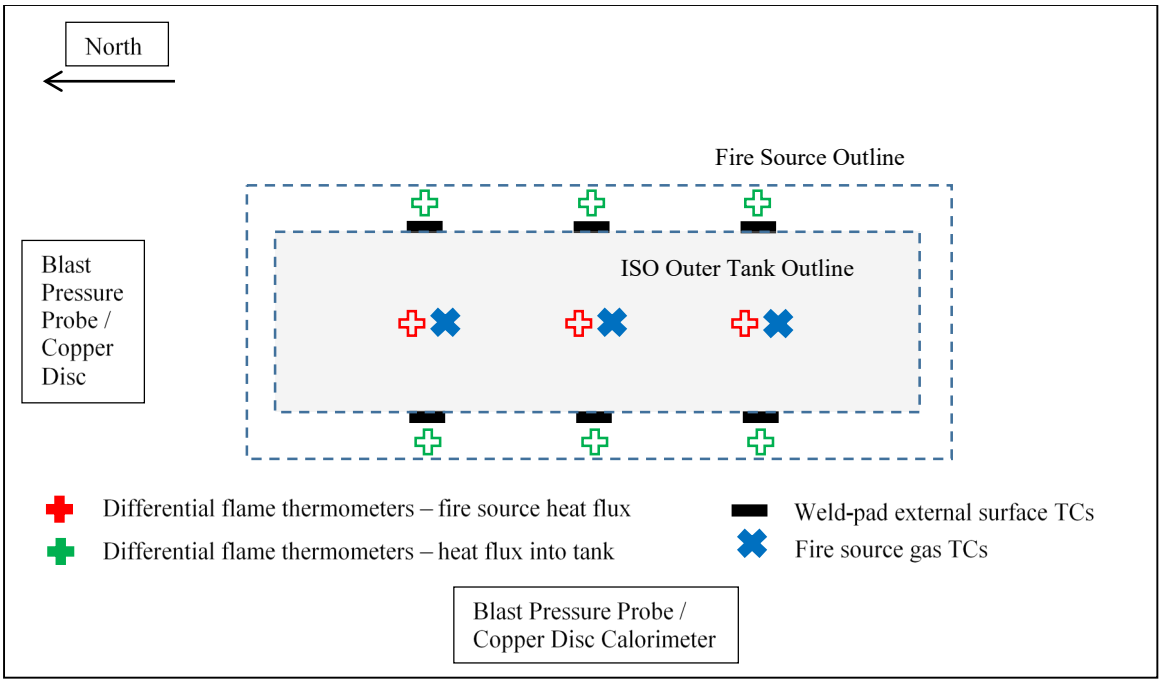

Figure 32. External Instrumentation Sketch

Figure 33 provides a similar plan view with distances to cameras and instrumentation. Figure 34 and Figure 35 provides details in elevation view of the location of weld-pad TCs and DFTs.

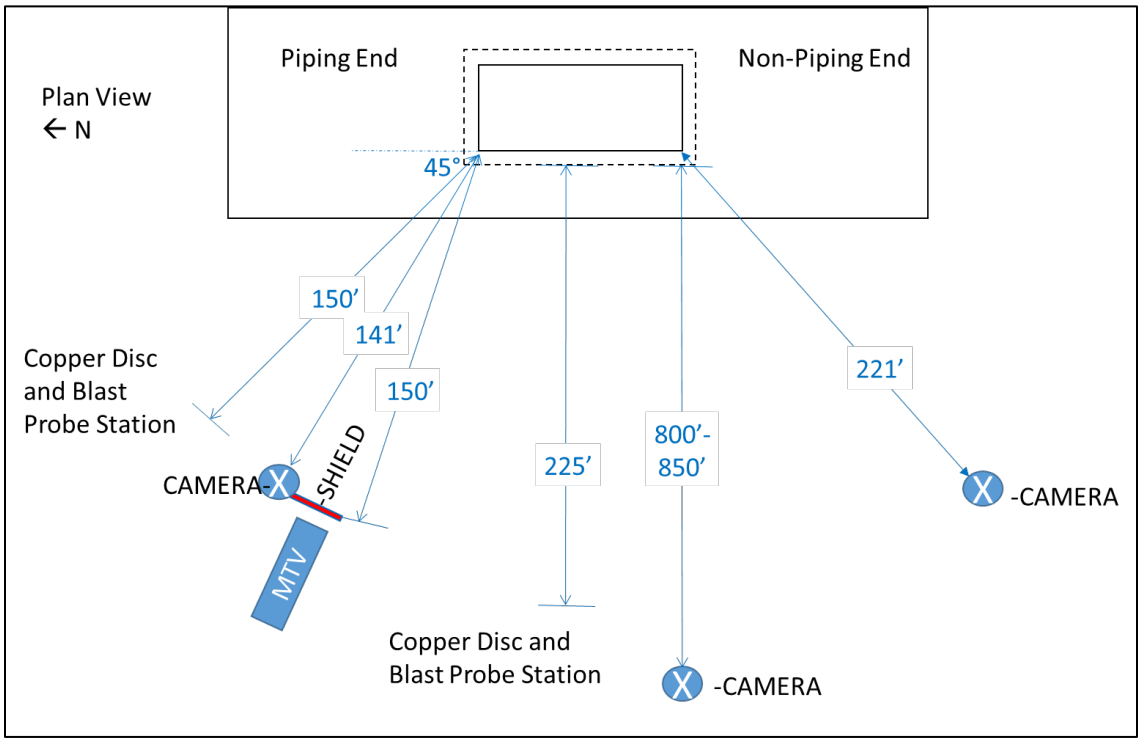

Figure 33. External Instrumentation Sketch (nominal distances to cameras and instrumentation)

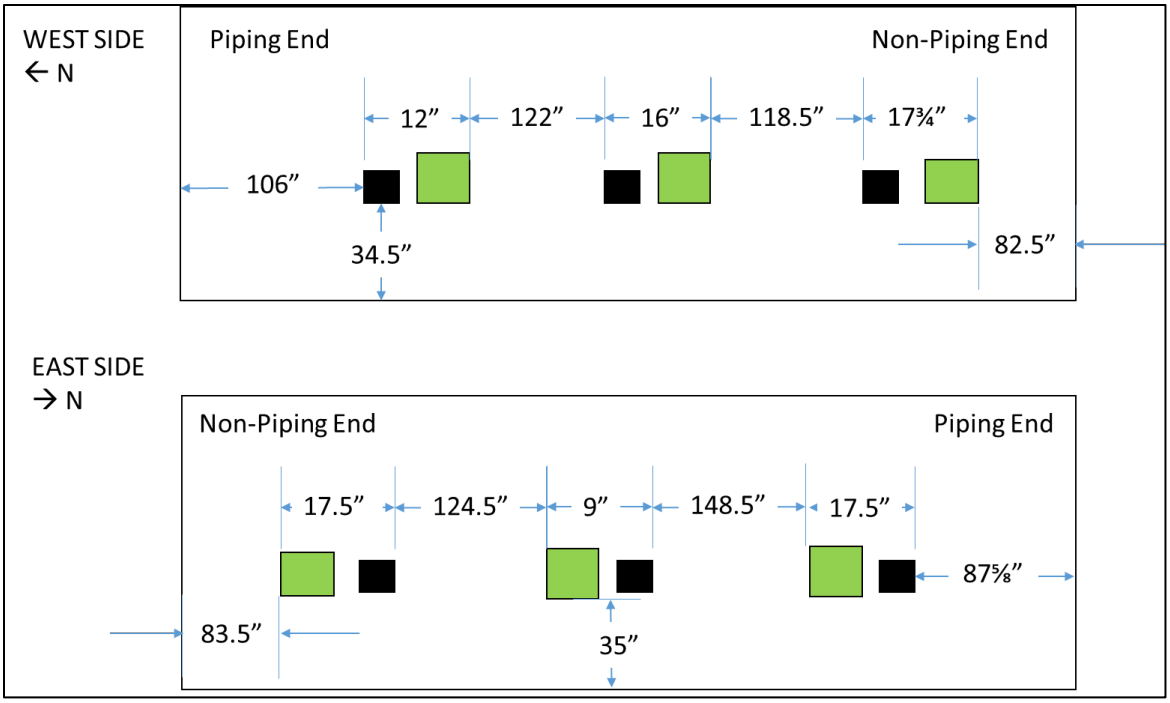

Figure 34. Weld-Pad TCs (black squares) and DFT Locations (green squares) – Elevation View from the East and West

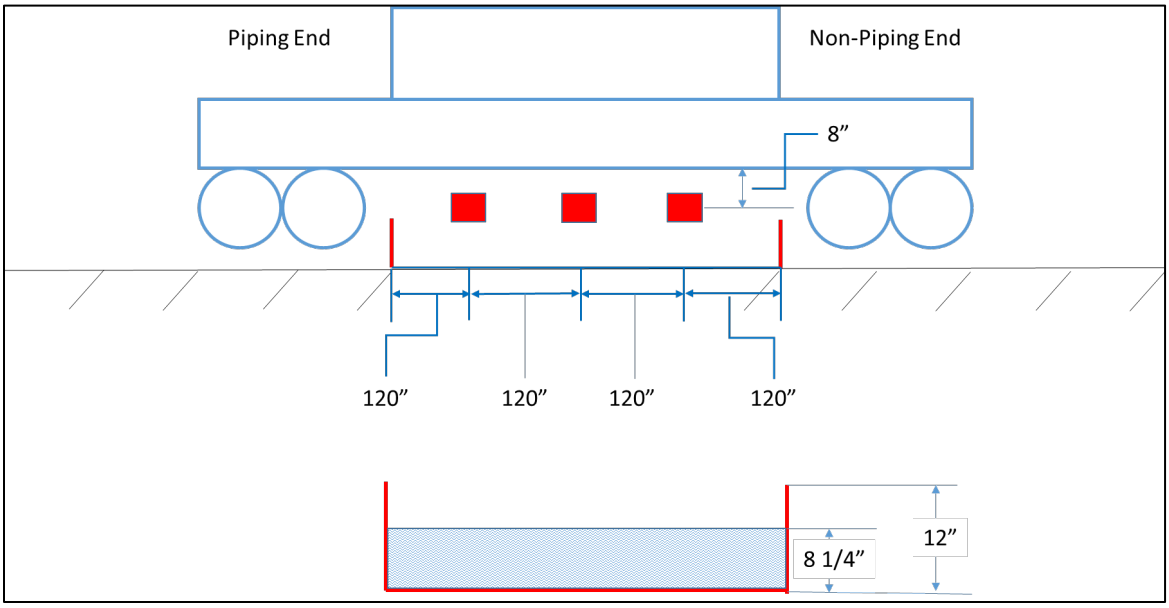

Figure 35. Fire Source DFT Locations (red squares) and Burner Pan Dimensions (elevation view)

6. Test Results

SwRI's Fire Technology Department performed a fire test of an LNG cryogenic tank (filled with LN2) secured on top of a flatcar on May 11, 2017, at SwRI's remote test site in Sabinal, TX. The tank was exposed to the fire source for a total of 2 hours, 35 minutes.

The following sections provide selected photographs of the setup, testing and post-test conditions, a summary of the video observations, a summary of the test data, and post-test observations and recommendations.

6.1 Selected Photographs

Figure 36 through Figure 39 show the test setup, pre- and post-test condition of the tank. Additional photographs and processed video of the test from each of the three camera angles have been sent to FRA.

	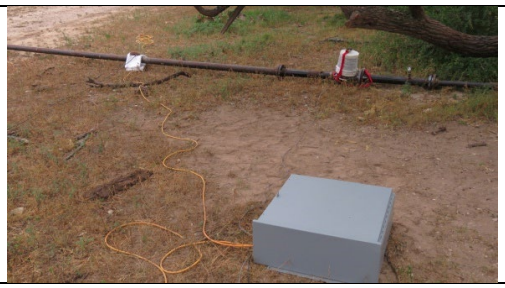
LPG Supply Tank, Pump and Bypass	LPG Flow Meter and DAQ
	
ISO Tank as Viewed from LPG Source	ISO Tank (East Side)
	
ISO Tank (West Side)	ISO Tank (North Side)
	
ISO Tank (South Side)	Instrumentation Trailer (NW of ISO Tank)
	
Valve Cabinet	Valve Cabinet

Figure 36. Selected Setup and Pre-Test Photographs

	
Test in Progress (View from LPG Supply Tank)	Test in Progress (Close-Up View)
	
Test in Progress (PRV Operating)	Test in Progress (PRV Operating)

Figure 37. Selected Testing Photographs

	
Post-Test: ISO Tank (East Side)	Post-Test: ISO Tank (West Side)
	
Post-Test: ISO Tank (North Side)	Post-Test: ISO Tank (South Side)

Figure 38. Selected Post-Test Photographs

	
Flatcar Buckling into Burner	Damage in Burner Piping Array
	
Flatcar Buckling into Burner	Flatcar Buckling into Burner
	
Post-Test: Valve Cabinet	Post-Test:Vacuum Pressure Damaged Connection

Figure 39. Additional Selected Post-Test Photographs

6.2 Video Observations

Table 5 summarizes the test observations recorded during the test and Table 6 summarizes the results of test observations of the synchronized video recordings.

Table 5. Summary of Test Observations Taken During Test

Time (h:min:s)	Observations
0:00:00	Start DAQ/cameras
0:11:13	Lit torch
0:12:05	Liquid propane flow initiated
0:12:16	Burner ignited
0:14:58	Vacuum pressure increasing
0:21:00	Tank pressure and vacuum pressure increasing; flame pushed to west side by wind
~0:24:00	Valve cover melting
0:33:45	Vacuum pressure signal lost
0:37:45	Vacuum pressure signal has returned, but may not be reliable
0:49:19	Some type T TCs seem to be losing connection
0:56:23	All type T TCs are unresponsive
1:00:00	Internal pressure is increasing
1:05:58	Internal pressure reached 114 psig
1:06:00	First PRV opened; later resealed
1:10:00	First PRV reopened (~116.5 psig internal pressure)
1:15:00	PRV pressure increasing, but tank pressure also still increasing
1:20:00	Noticed flatcar is bowing downward
1:28:00	Visual PRV venting, but pressure still increasing
1:30:00	No change
1:33:38	Second PRV opened (~155 psig internal pressure)
2:45:00	Liquid propane flow shut off
2:46:58	Burner fire self-extinguished
2:51:00	Stopped DAQs (restarted high-speed DAQ to record cool-down)

Table 6. Summary of Test Observations from Synchronized Video

Time (h:min:s)	Observations
-0:01:17	Test video begins
-0:01:02	Ignitor in center of pan is lit and the site is cleared downrange
-0:00:07	LPG flow initiated and bubbling can be observed through water substrate
0:00:00	LPG ignition observed – START OF TEST
0:00:33	Flames independently burning at first rib on side of tank, likely consuming exterior paint on tank
0:00:43	Flames on tank extinguish themselves
0:01:09	The tank appears to be adding to the fire source, but could also be an increase in LPG flow rate
0:01:41	Walls of cylindrical part of the tank sustain flames
0:01:46	Gases seen coming from tank from its cylindrical walls, likely related to rapid warming of tank
0:02:10	Additional flaming of tank walls at NW corner of tank
0:03:45	Gases continue to be observed coming off the tank and being entrained into fire
0:04:22	Flames are visible inside piping cabinet
0:04:59	Piping end (north) tank cap is severely charred
0:05:07	Flames are sustained on left tank cap
0:08:08	Flames are sustained on the right tank cap
0:08:25	Flames on right tank cap extinguish
0:10:56	Something happens at the center of the fire source and it begins to split in two sections
0:11:08	Fire momentarily clears at center of tank, interesting black discoloration line along top of tank
0:11:50	Fire is now burning in two concentrated areas with a gap between them in the center of the pan. Intermittent jets of gas can be seen around the center of the pan – this could have been a possible failure of part of the burner connections
0:13:20	Ripples seen on cylindrical wall of the tank
0:14:10	Fire from pan burning at both ends of the pan; the center of the tank sustaining flames
0:16:00	Pan fire burning evenly from end to end
0:18:00	Status unchanged
0:21:00	Status unchanged
0:23:45	North 1/4 of tank sustaining flames
0:24:10	North 1/2 of tank sustaining flames
0:25:45	Center of tank sustaining flames
0:30:00	Flame height/density diminishes
0:35:00	Status unchanged
0:37:15	Flame height/density increasing
0:40:00	Flame intensity high on right side of tank
0:40:45	Flames visible from back side of tank
0:41:18	Left side is engulfed on both near and far side of railcar
0:42:20	Smoke flowing from back side of tank

Time (h:min:s)	Observations
0:43:20	Flame intensity low on north side, high on south
0:45:10	Flames seen over the top coming from far side (east) of tank
0:46:12	Flames seen coming over the top of the tank equal height to those in front, located approximate center of tank
0:47:00	Flames engulfing center of tank from both east and West side
0:47:40	Heavy flaming on far (East) side of tank
0:48:30	Flame intensity is high on near (West) side of tank, flames seen over the top coming from the far (East) side of the tank
0:48:40	Smoke thickens, now is a darker smoke being released
0:49:30	Smoke thickens, black plumes released from fire
0:51:30	Smoke thins out momentarily
0:51:50	Thick smoke returns, black plumes observed
0:53:50	Status unchanged
0:54:35	Flaming visible on flatcar floor
0:55:25	High intensity flaming on both near (West) and far (East) side of railcar
0:56:00	Smoke intensity increases
0:56:58	Combustion gases flowing from top of tank
0:57:15	Smoke intensity increases
0:57:30	Smoke release rate increases
0:58:50	Smoke thins and smoke release rate decreases
1:00:00	Smoke thick again, high smoke release rate. Source is both front (West) and back (East) of tank. Railcar floor is getting lower. Significant difference from the start
1:10:00	Heavy smoke, fire on both sides of tank
1:11:30	Heavier smoke
1:18:21	PRV activates
1:19:17	PRV closes
1:19:29	PRV re-activates
1:19:54	PRV still open; highest exhaust rate occurring now
1:20:06	PRV still open; exhaust rate decreases
1:21:20	PRV still open; exhaust rate increases to max for approximately 3 seconds before decreasing again
1:22:20	PRV still open; exhaust rate hits max again
1:22:30	PRV closed
1:22:39	PRV open
1:23:25	PRV closed
1:24:15	Thick black smoke exhausting from fire
1:26:13	PRV open in small spurts
1:26:56	PRV open and releasing more visibly
1:29:57	PRV closed
1:30:10	PRV open
1:31:15	PRV closed
1:31:38	PRV open

Time (h:min:s)	Observations
1:32:09	PRV closed
1:32:27	PRV open
1:32:53	Thick smoke blocks view of PRV
1:33:20	PRV seen open in small spurts
1:33:45	PRV opens and releases pressure rapidly
1:36:18	PRV closed
1:36:55	PRV open
1:44:03	PRV abruptly closes then reopens seconds later
1:49:44	Flame spreads to circular face on the right (south) side of the tank; flame intensity increases on this side of the tank
1:54:30	Circular face on right (south) side of tank is black from charring; combustion gases release from tank on this side
2:15:00	Unchanged; PRV open
2:17:12	PRV closed, smoke accumulates to the left (north) of the railcar
2:17:38	PRV opens, smoke clears
2:18:30	Tank releasing combustion gases on right (south) side, smoke from fire thickens/blackens
2:23:00	Status unchanged; PRV open
2:30:00	Status unchanged; PRV open
2:31:50	PRV closed
2:32:10	PRV open
2:33:30	Fire dies down
2:34:00	Fire mostly extinguished, only burning in a small center area close to ignition location
2:40:05	Fire completely extinguished; PRV remains open
3:30:00	Gases escaping at edge of circular cap
3:56:50	More gas escaping
3:57:15	More gas escaping; more or equal to the gas released from PRV
4:10:00	Status unchanged
4:22:15	PRV closed; gas escaping from cap edges
4:36:39	PRV open; gas still escaping from cap edges
4:50:55	PRV closed; gas still escaping from cap edges
5:05:38	PRV open; gas still escaping from cap edges
5:16:40	PRV closed; gas still escaping from cap edges
5:31:40	PRV open; gas still escaping from cap edges
5:41:07	PRV closed; gas still escaping from cap edges
5:56:29	PRV open
6:04:27	Video end—tank still venting

6.3 Post-Test Observations/Findings

The day after the test on May 12, 2017, SwRI staff accessed the test site and inspected the tank. Conditions were determined to be safe to approach the tank based on the pressure and temperature data as well as the hand-held oxygen sensors. The following observations were made based on the post-test inspection.

- The tank successfully vented its contents and did not rupture.
- The tank kept venting overnight and was at atmospheric pressure the next morning.
- When the flatcar started to buckle, it sank into the burner and impacted the piping, which contributed to burner performance.
- At this same time, some of the tank instrumentation—DFTs on the sides of the tank—pulled away from the tank slightly.
- Researchers visibly confirmed that the fire damaged the vacuum pressure cable. This would be a point of emphasis in terms of how to take this measurement more robustly in the next test. They also confirmed that the tank lost its vacuum. This was checked by opening the valve at the top-right of that end of the tank, which is the port used to pull the vacuum by the manufacturer. When this valve was opened, there was no indication of a vacuum in the annular space (i.e., no suction was heard or felt by operator).
- The two 6-inch "pancake" pop-off valves on the non-piping end of the tank did not blow off, but were visibly loose, so it was likely that they both activated. This was consistent with losing the vacuum in the annular space. Since these did not blow off violently, it was not possible to determine the exact time from the review of the video.
- The type T thermocouple connections did not appear to sustain a lot of damage, as originally thought, when these channels began to stop responding during the test. It may have been possible that there was an internal shorting-out of these pass-through connectors, as opposed to external damage. This still requires additional analysis and will need to be considered in the details of the test design for the next test.

6.4 Data Summary

Figure 40 through Figure 42 provide temperature and heat flux data, as determined from the DFTs on the side of the tank and over the fire source. Figure 43 shows the incident heat flux data, as determined from the copper disc calorimeters. Figure 44 shows the internal and external tank temperatures as well as the various tank pressures and wind speed during the test. Figure 45 shows the cool-down temperatures and pressures. The tank safely vented its contents and did not rupture, so no blast pressure data was collected.

Temperature Graph	Heat Flux Graph
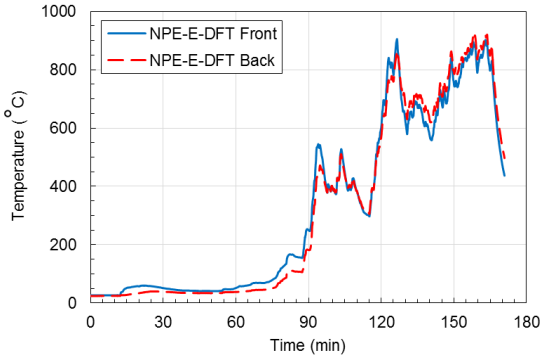	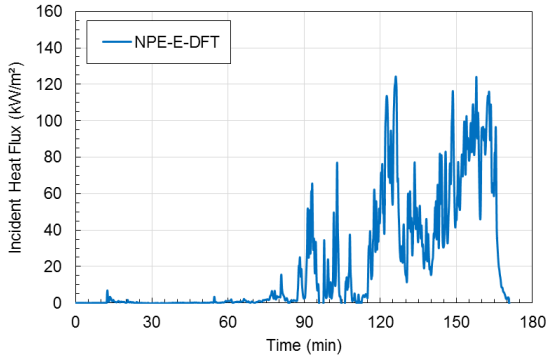
Non-Piping End – East - DFT	
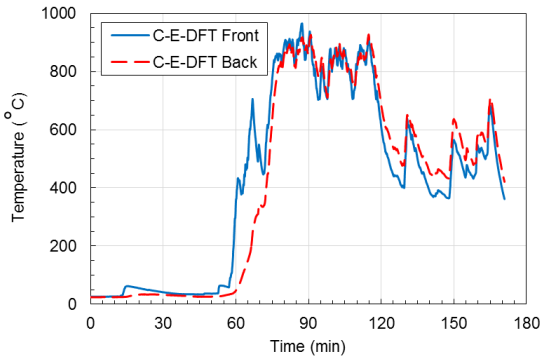	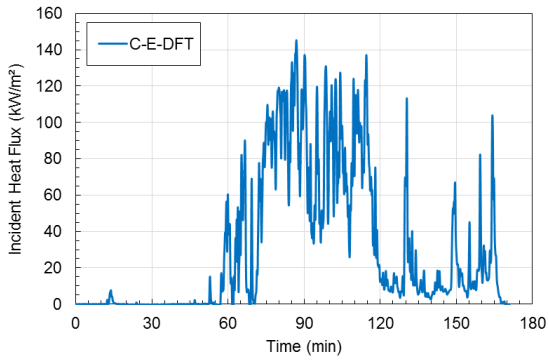
Center – East - DFT	
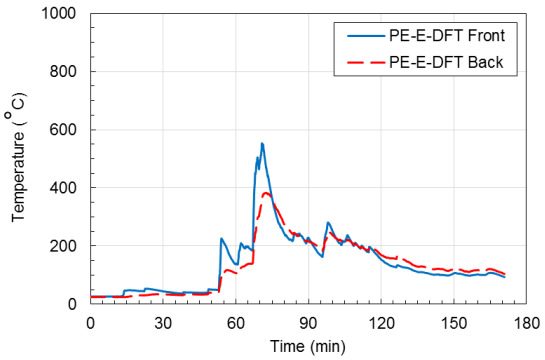	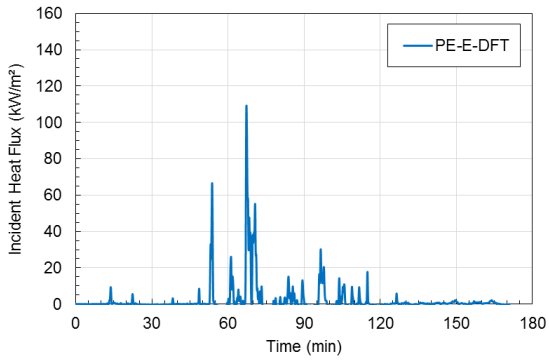
Piping End – East - DFT	

Figure 40. Temperature and Heat Flux Data from East Side of Test Tank

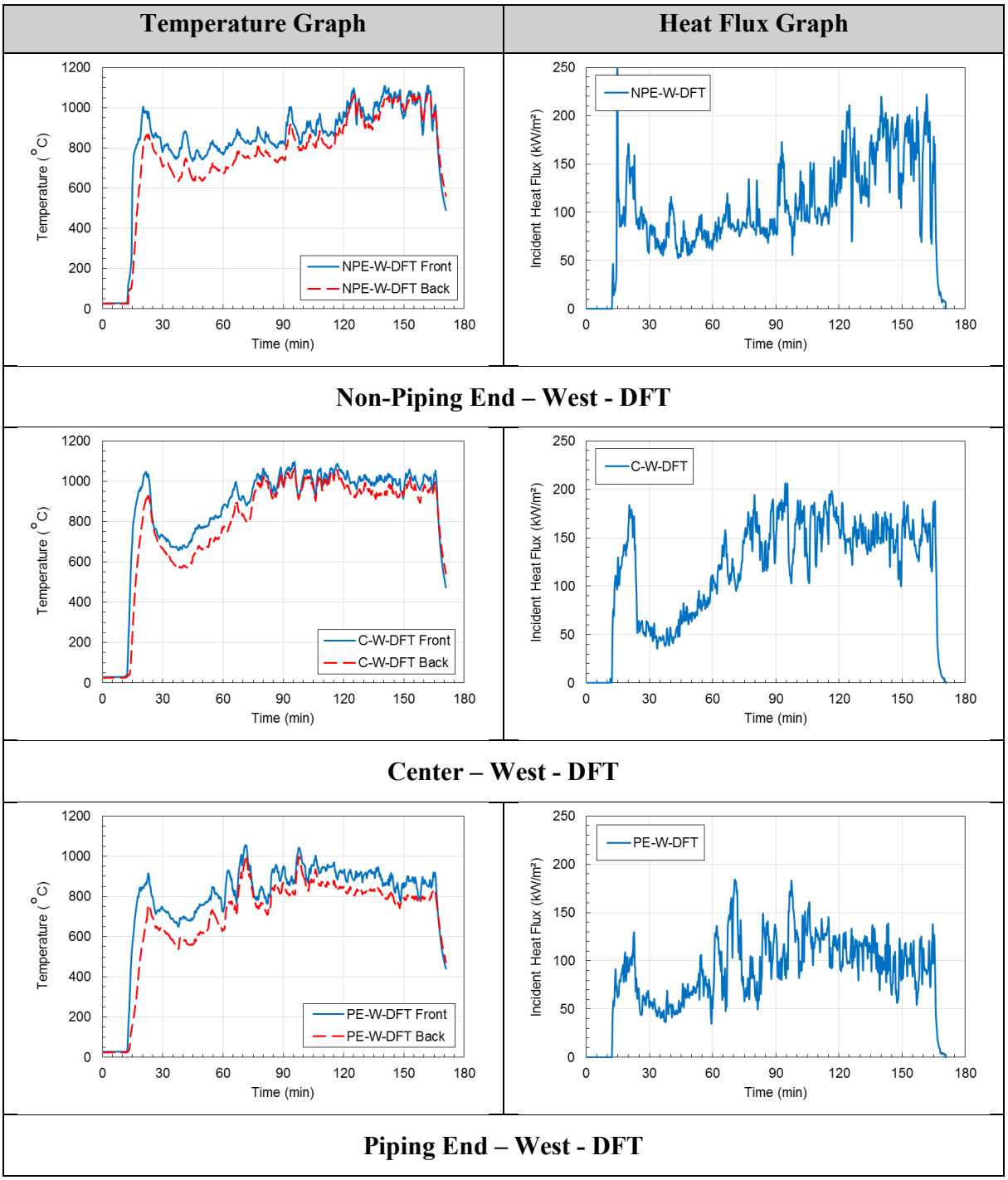

Figure 41. Temperature and Heat Flux Data from West Side of Test Tank

Temperature Graph	Heat Flux Graph
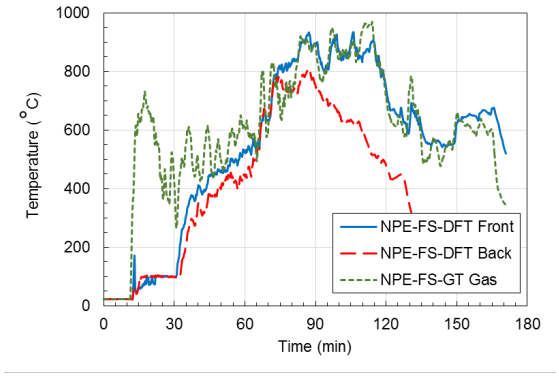	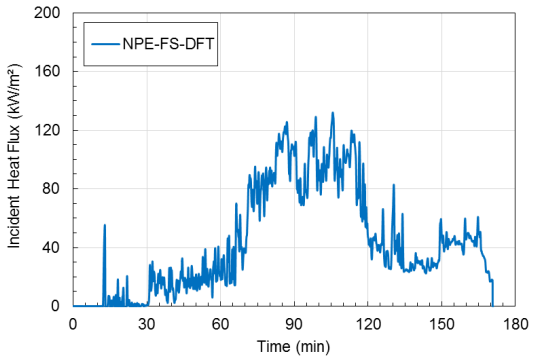
Non-Piping End – Fire Source - DFT	
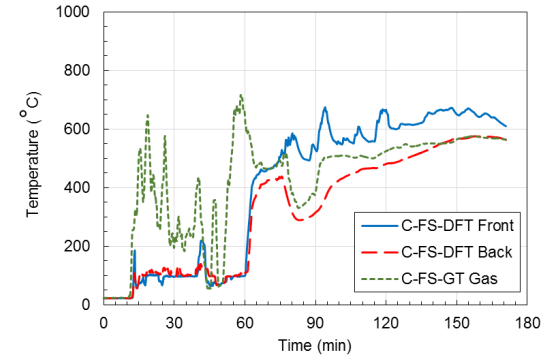	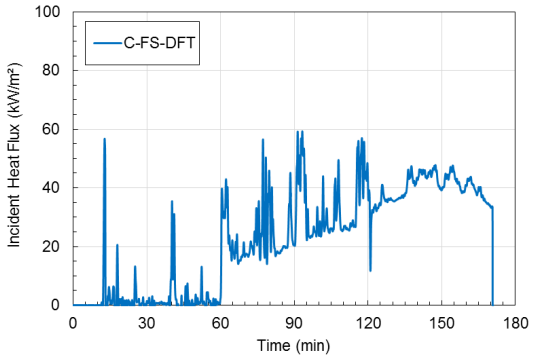
Center – Fire Source - DFT	
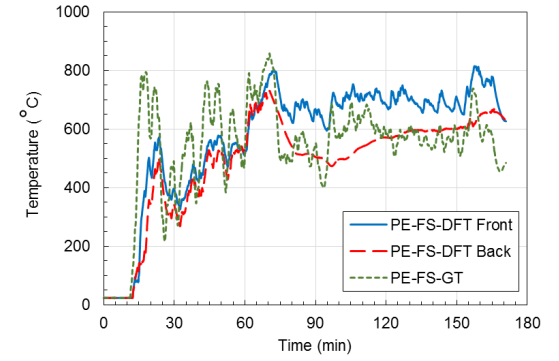	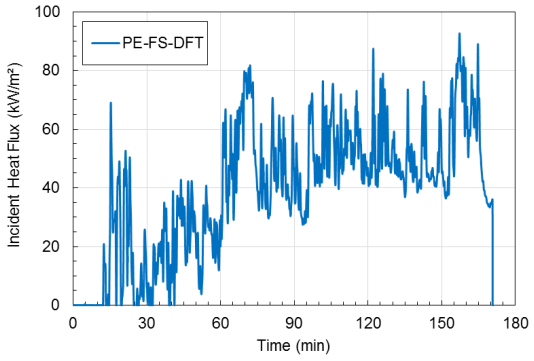
Piping End – Fire Source - DFT	

Figure 42. Temperature and Heat Flux Data from the Fire Source

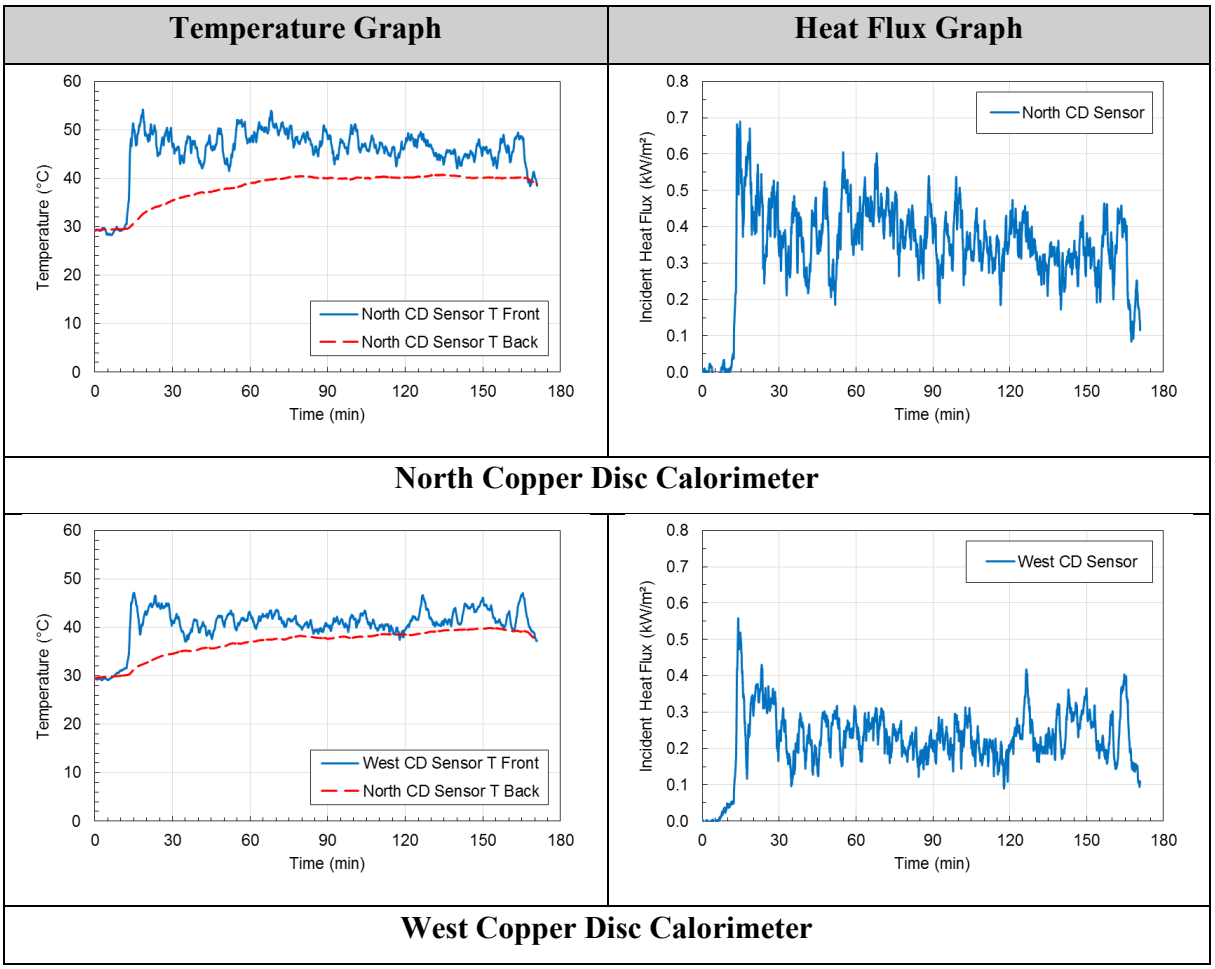

Figure 43. Incident Temperature and Heat Flux Data from Copper Disc Calorimeters

Figure 40 and Figure 41 show that the fire exposure to the tank was not uniform—likely caused by wind conditions. This resulted in a more severe exposure on the west side of the tank, as compared to the east side. The average peak incident heat flux to the east side of the tank was 127 kW/m^2, and the average peak incident heat flux to the west side of the tank was 207 kW/m^2.

In Figure 42, the average peak incident heat flux from the fire source to the bottom of the flatcar was 95 kW/m^2 and was higher on the "edges" than in the center. The most likely reason that the heat flux measured close to the fire source was lower than that measured on the sides of the tank was due to a lower concentration of oxygen in the region between the fire source and the bottom of the flatcar, as opposed to just above the flatcar, where there was more oxygen available for combustion. In addition, since the flatcar sagged due to the exposure, at some point during the test, the center DFT was submerged into the burner and this phenomenon was exacerbated.

Figure 43 shows the incident heat flux to targets 38–69 meters (125–225 ft.) away was quite low and consistent with background incident radiation from the sun on a warm day in South Texas.

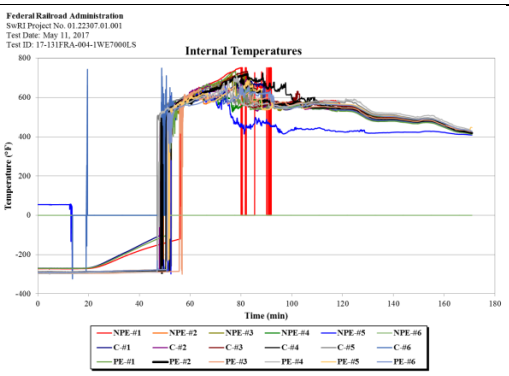

Internal Tank Temperatures

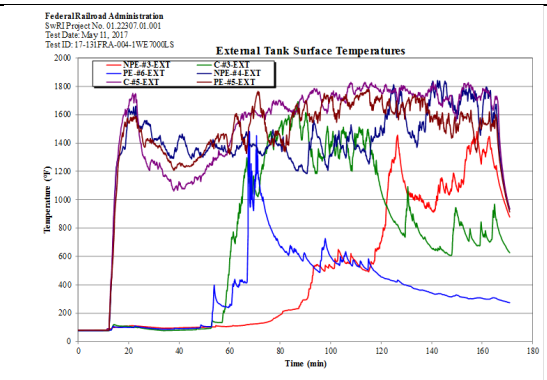

External Surface Tank Temperatures

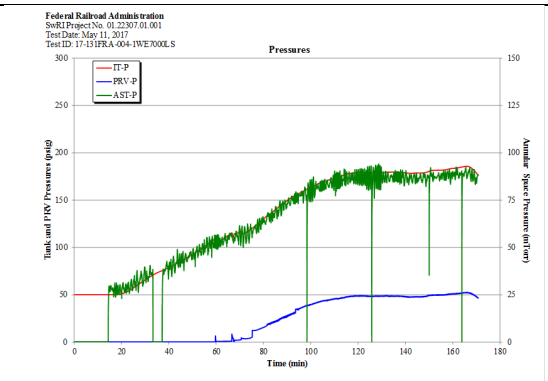

Internal Tank Pressures

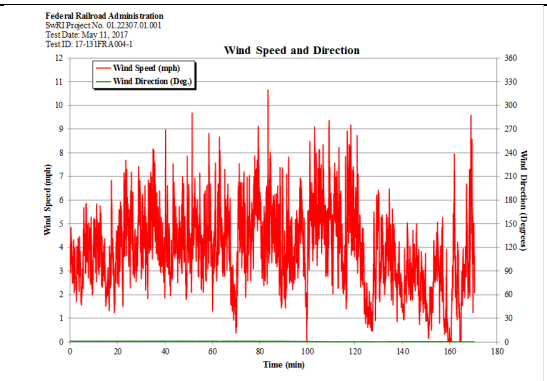

Wind Speed During Testing

Figure 44. Internal and External Temperatures as well as Pressure Data, Propane Flow Rate, and Wind Speed Data

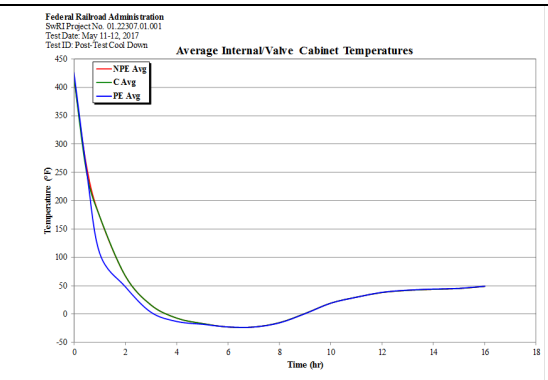

Average Internal Temperatures

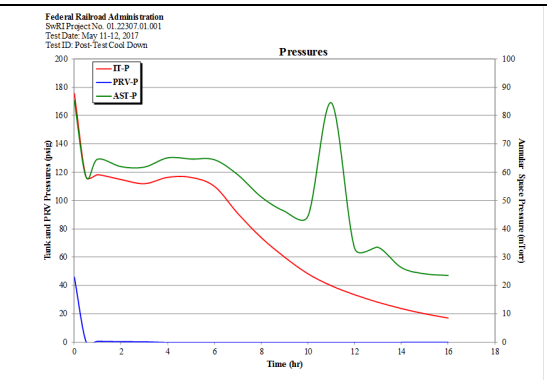

Internal Tank Pressures

Figure 45. Selected Cool-Down Data

Figure 44 (also see Figure 45) illustrate how the internal temperatures and pressure increased during the fire test. Unfortunately, the signals to all of the internal TCs were lost after the first 45 minutes of the test. During this time period, the highest (in elevation) TCs rose from approximately -132 °C (-270 °F) to -38 °C (-100 °F). These TCs were in the vapor space of the tank and indicated how the gas temperature in this region was increasing due to the fire exposure. The graph indicates the temperature rise for the rest of the internal thermocouples; however, the specific data was compromised due to the fire exposure damaging the connections within the piping connections.

The PRVs seemed to operate at the correct nominal pressure. Figure 45 shows the first large increase on the PRV-P channel occurred at an internal tank pressure of approximately 803 kPa (116.5 psig), which coincided with the first PRV stated set pressure of 793 kPa (115 psig). The second large increase on the PRV-P channel occurred at an internal tank pressure of approximately 1.068 MPa (155 psig), which coincided with the second PRV stated set pressure of 1.034 MPa (150 psig).

In Figure 45, average valves are provided to demonstrate the cool-down of the tank over the 16 hours after the termination of the test (until the next morning). The tank slowly cooled and bled all the remaining LN2 through the night and reach ambient conditions by the following morning when personnel arrived again at the test site.

7. Modeling Results

The following sections provide additional information about the computer modeling performed to support the analysis in Phase 1 of this project.

7.1 General Discussion of Methodology

The quarter FE model described in Section 3.3 was used to investigate the effects of thermal loading from a pool fire on tank wall temperature, LNG temperature, interior tank pressure, and tank wall failure. The structural strength of steel deteriorates under high temperatures, though the effect of this phenomenon is not well known or documented with regard to LNG tank performance in pool fires. Likewise, the complex relationship between interior temperature, pressure, and LNG phase and the wide variations in temperature across different boundaries of liquid, gas, and solid materials is unknown. The model was used to investigate these unknowns.

The quarter tank model was subjected to a thermal loading environment representative of a pool fire for 1 hour. The thermal conductivity value for the insulation was varied over multiple simulations to characterize the range of performance capabilities expected under such conditions. Initial temperatures were assigned to each part corresponding to a standard operating environment. A convective heat transfer boundary condition was prescribed to the exterior surface of the outer tank to simulate the thermal loading due to the pool fire.

The meshes representing different parts in the model were connected with merged nodes, except for the fluid contacts (LNG and air) and the inner tank. These were connected via a thermal contact definition using 2.0 W/m-K as the thermal conductivity for the baseline run. The tank material was defined with temperature-dependent properties for conductive heat transfer. The thermal conductivity value for the insulator was altered over two simulations to determine the magnitude of its effect. A third simulation was conducted in which radiation-induced heat transfer functionality was turned on in the model. The steel support rings were changed to an ideal insulating material for the second simulation. Natural convection inside the LNG and air cavity parts was ignored for simplicity. The thermal conductivity values specified for each part were based on published values or proprietary information supplied by the tank manufacturer.

7.2 Results

The temperature time history was calculated for each part along a vertical path at the midspan of the tank as shown in Figure 46. The temperature time histories for each simulation are provided in Figure 47 through Figure 49. A fringe plot of the final temperature for the simulation with radiative heat transfer, corresponding to Figure 49, is depicted in Figure 50. The LNG temperature remained fairly constant throughout the entire 60 minutes, regardless of insulator thermal conductivity value. Changing the support rings from steel to an ideal insulator greatly reduced the heat transfer between the outer and inner tank.

As identified in the 53-day simulations, the tank temperature response, especially the inner tank, was significantly affected by the insulator characteristics. This highlighted the need to accurately define the performance characteristics of the insulator over the range of temperature and pressure conditions expected to be encountered in a fire event. Insulator performance can vary widely with pressure and/or temperature changes such that its thermal conductivity can

increase by an order of magnitude or more if vacuum conditions are not maintained. It is expected that the pressure and temperature of the insulation volume between the inner and outer tanks will increase significantly due to external heating; these effects should be investigated.

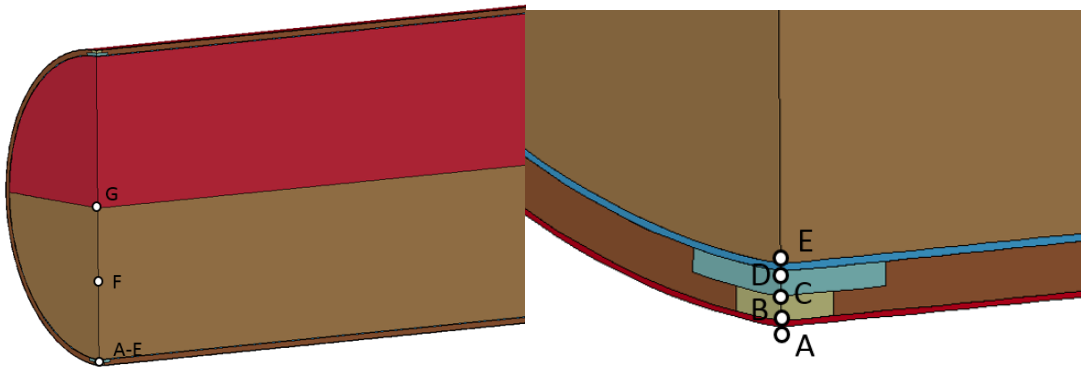

Figure 46. Model Temperature Measurement Locations

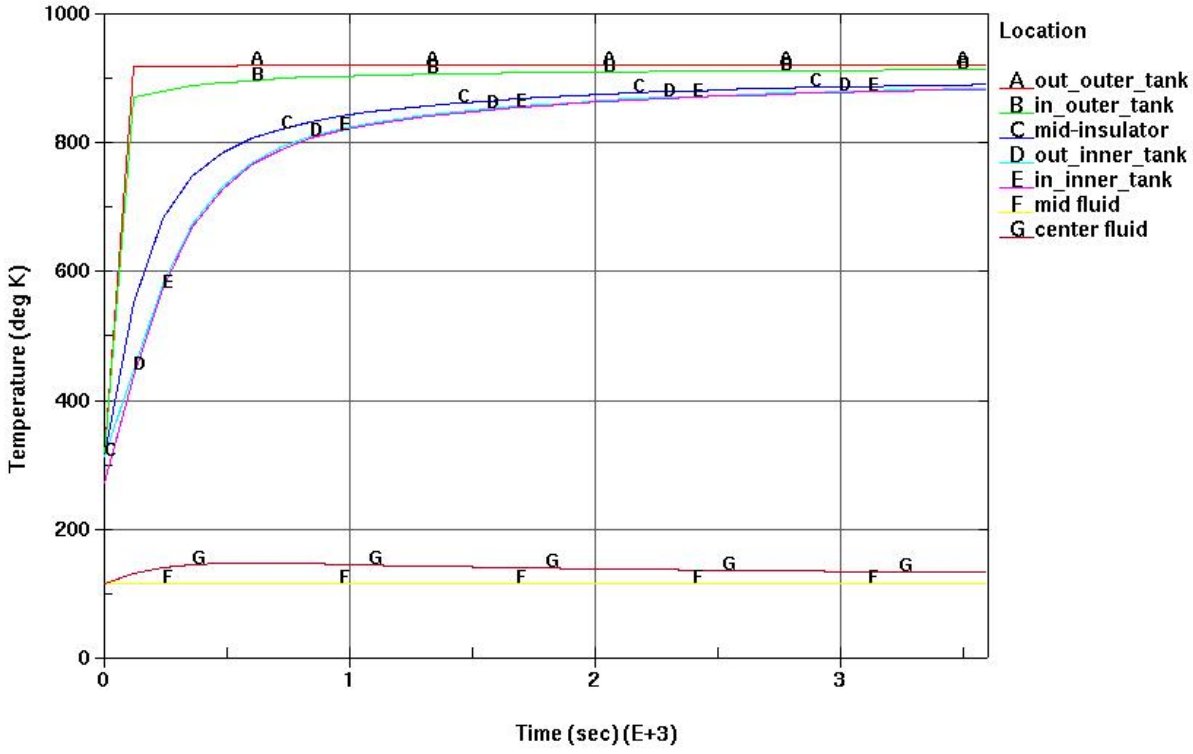

Figure 47. Temperature Time History; Realistic Insulation

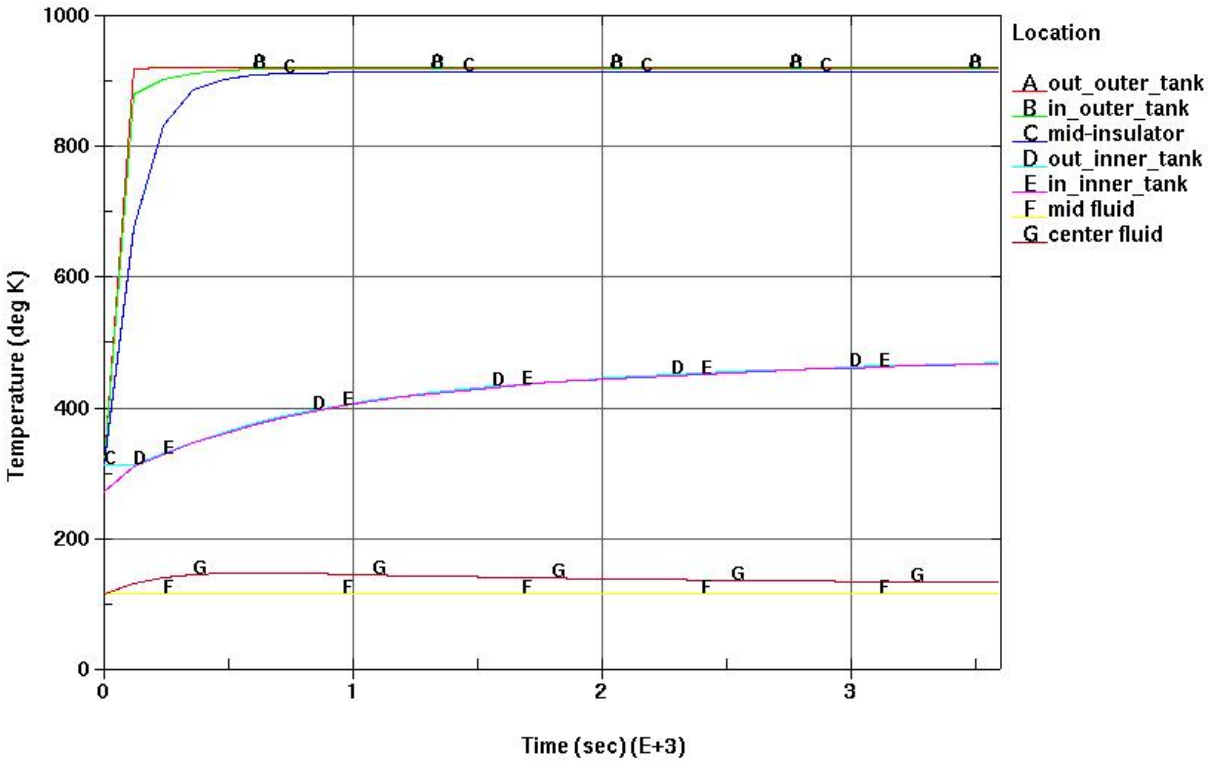

Figure 48. Temperature Time History; Ideal Insulation, Non-Steel Support Rings

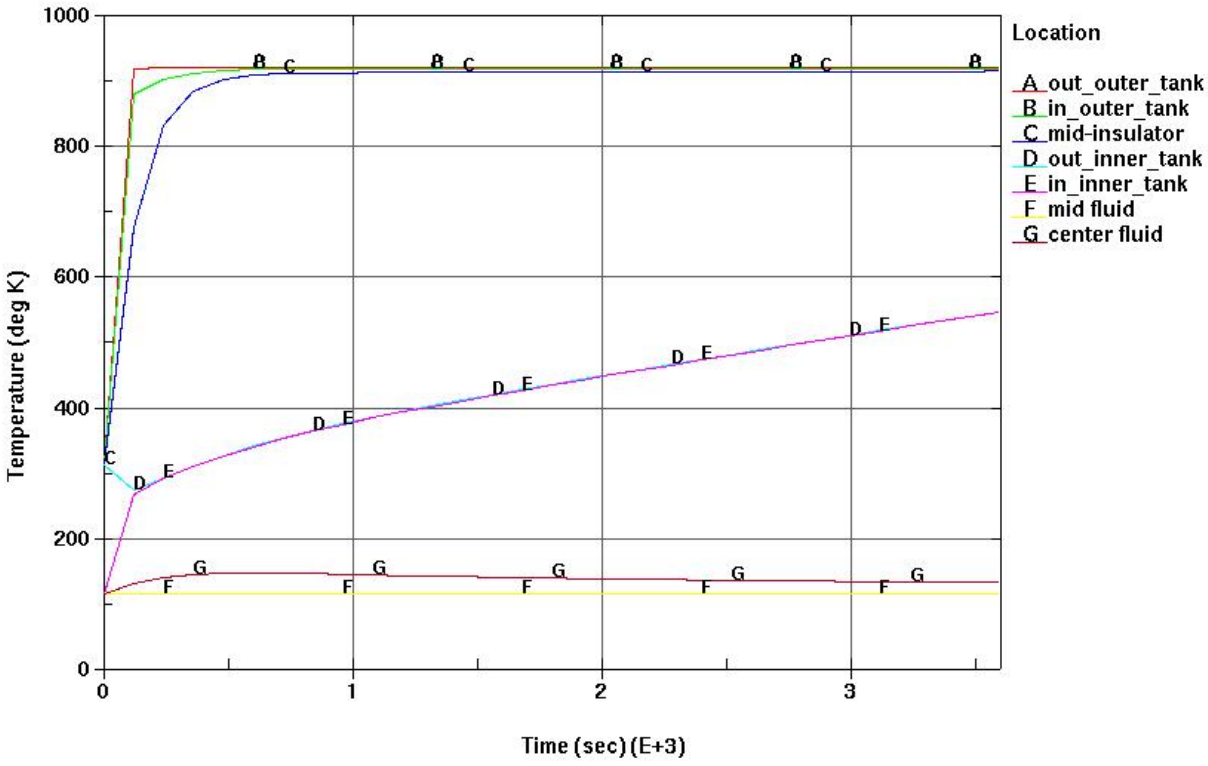

Figure 49. Temperature Time History; Incorporating Radiative Heat Transfer

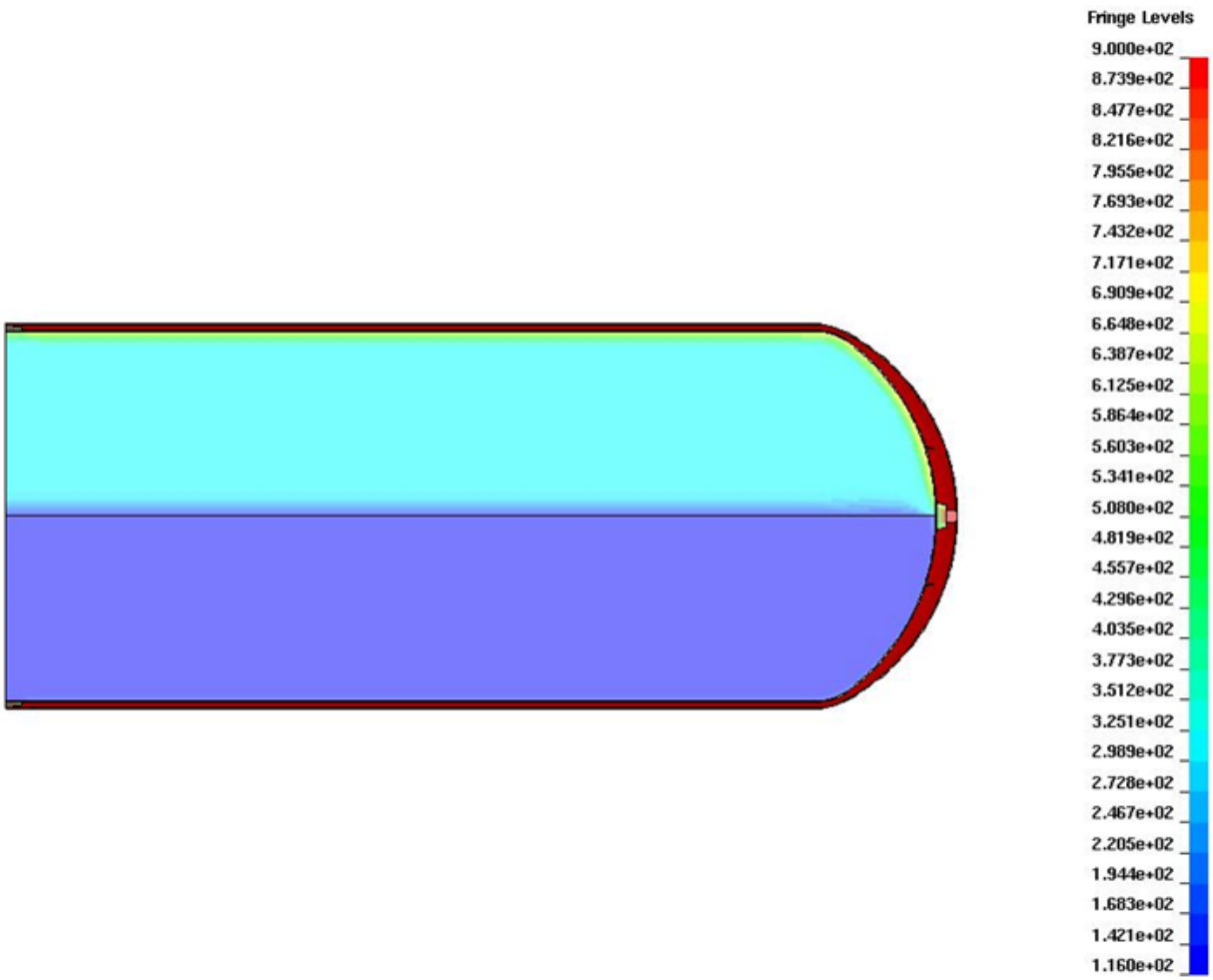

Figure 50. Fringe Diagram of Temperature in Tank Model Incorporating Radiation Heat Transfer

Additional simulations were conducted to evaluate the effect of tank temperature on tank structural performance to the point of catastrophic failure. Two simulations were conducted, both with linearly increasing pressure applied to the inner tank, and constant temperature applied to all parts. In one model, an ambient temperature was applied to all parts. In the second model, the temperature of each element was defined to correspond to the end of the 1-hour thermal load simulation (pool fire scenario) in the third model described above (Figure 49 and Figure 50).

The results of the simulation indicated that tank temperatures representative of those generated in a fire scenario would result in the tank failing much earlier, at approximately half of the maximum pressure, than if it were at an ambient temperature.

8. Conclusion

The following sections highlight a few conclusions from the testing and modeling activities during Phase 1 of the project.

8.1 Testing

- An ISO Tank, filled with LN2, was exposed to a LPG fire for 2 hours, 35 minutes.
- There was no rupture or BLEVE of either the inner or outer tank.
- The steel in the rail car exceeded its softening temperature. The rail car sagged downward until it was supported by the fire pan.
- Based on the internal pressure rise, the insulation degraded in the fire relatively quickly. It was expected that the thermal properties of the insulation material would greatly affect the performance of the tank in a fire scenario.
- The pressure inside the inner tank increased monotonically during the fire exposure and stabilized at approximately 180 psig.
- The PRV system worked properly. The lower pressure (114 psig) valve opened and reseated twice and then opened fully. The higher pressure valve opened at about 150 psig. The pressure continued to rise until 180 psi and the venting stabilized.
- There was additional venting after the fire exposure stopped, and this continued for more than 3 hours, 40 minutes (extent of video footage after fire exposure finished).
- The morning after the test, the internal pressure in the tank was nearly atmospheric, there was no visible venting of the remaining LN2 in the ISO tank, and there was no vacuum in the annular space.
- The venting orientation/direction could be important in the field. The venting jet on this tank would impinge on a joining ISO tank or rail car. The ISO tanks might also be stacked. If tested with LNG, this vent would be like a torch and could spread the fire to neighboring tanks.

8.2 Modeling

- The temperature of a tank will greatly influence the failure pressure of that tank. The failure pressure for a heated tank has been shown to be much less than that of a tank at ambient temperature.
- The preliminary modeling results suggested that additional effort should be applied to assessing the potential failure of the tank under elevated temperatures.
- The preliminary modeling results suggested that additional effort should be applied to accurately characterizing the thermal insulation properties as well as vacuum retention capabilities of the annular space under thermal loading.
- The introduction of phase change into the modeling needs to be accomplished to better understand the various mechanisms that are involved during the heating process.

- Studying the effect of wind, flatcar geometry, and burner size on the heat flux to the tank should be expanded so as to better understand the effects of conditions that may be present at the physical test.
- The results obtained in the test should be utilized to validate the models developed in the next phase of this project.

9. Future Work

The following sections provide recommended future work related to testing and modeling topics of Phase 1 of this project.

9.1 Testing

The following subsections provide recommended future work related to testing.

9.1.1 Additional Analysis of Phase 1 Data

A substantial amount of data was collected during the full scale LN2 test. In a future task, the data will be analyzed with an eye for the implications future test preparations. For example, the following subtasks could be completed:

- Determine how much LN2 was left in the tank at the end of the test
- Determine the flow out of the PRVs as a function of time and internal pressure
- Analyze heat flux that was applied to the tank
- Analyze the fire test results and cool down test data
- Correlate the test data with the video images of the fire orientation due to wind using the three video cameras
- Determine the total heat release applied to the tank and that which was generated by the propane
- Identify the internal tank conditions through the course of the test
- Analyze multiple samples from the tank outer wall (areas thought to be the hottest and the coolest on the outer wall), insulation layer, and inner wall
- Quantify the degradation of the insulation material

In addition, the virtual testing analysis methods utilized to date could be compared with the test results. For example, the following subtasks could be completed:

- A comparison of heat fluxes that would be expected using the wind conditions at the time of the test, and the fluxes observed.
- A comparison of expected pressure given the heat flux applied incorporating phase change.
- The effects of shielding by the flatcar on heat flux applied.
- The effects of burner system damage on heat flux expected to be applied versus those that were applied.
- An analysis of burner performance, flow rates, and time until complete fuel consumption.

It could be beneficial to perform some forensic analysis of test hardware. For example, the following subtasks could be performed:

- Examine state of all valves and whether still functional
- Examine the insulation in the annulus and determine its state post-test
- Determine the state of the support structures of the inner tank
- Determine the state of the ISO frame for the tank
- Document the surface characteristics of the tanks and any white paint that still exists

9.1.2 Phase 2 Testing – LNG

The results of the post-Phase 1 tasks described above will help identify how expanding the coverage of the burner system will impact the expected thermal loads on the tank and will aid in evaluating the effects of alternative wind conditions on these results. The planning for the next test will also include the identification of potential wind countermeasure systems to control the effects of wind on heat fluxes to the test tank. Complete an analysis of the expected effects on tank materials, internal pressures, and fluid levels with full heat flux being applied to the LNG tank filled at various levels.

A test plan for LNG inside the test tank will be prepared, which will address the following topics.

- Test safety requirements for performing the test with the tank filled with LNG
- The ability for the formation of a vapor cloud from leaks
- The effects from ignition of LNG at PRV exhaust, including jet flame length and direction
- The effects of ignition on expected component performance
- Test parameter values predicting a BLEVE event that would enable test shutdown prior to event
- The potential for shock wave creation from a rupture event and subsequent effects under fire conditions
- Determination of the test site requirements and location that are appropriate for the test

The test will be carried out according to the test plan and analysis of the results will continue into Phase 3 of the project.

9.2 Modeling

The following subsections provide recommended future work related to modeling.

9.2.1 Validation of Analysis Methods

The test data generated from Phase 1 will be used to validate the various numerical models. As required, the models can be validated to match the performance of select outputs, such as but not limited to, internal temperature and pressure, boil-off rate, structural performance, and thermal loading conditions.

9.2.2 Incorporation of Phase Change

The tank model will be evaluated in a multi-physics numerical simulation environment that is capable of modeling chemical reactions, thermal loading, and shockwave initiation and propagation. This method will allow for the simulation of phase change effects according to the two-phase equations of state for LN2, LCH4, and LNG.

Key outputs will include a determination of internal pressure versus time and heat flux, the internal tank and fluid temperature gradient across the LN2, LCH4 and LNG phases, and an evaluation of the pyrolysis of the insulation and loss of vacuum. The properties of the tank material with respect to temperature will also be accounted for to ensure a valid representation of its strength, especially with respect to areas with large temperature gradients.

The rapid expansion of high temperature LN2, LCH4, or LNG at the time of catastrophic tank failure will also be modelled to evaluate characteristics relevant to a BLEVE event. The results will be compared with the available data from the test. The function of the PRVs will be incorporated and an evaluation of expected release times and volumes will be compared with the timing observed in the test videos.

9.2.3 Evaluation of Crashworthiness

Direct structural damages due to crash circumstances will be assessed with regard to the possible failure modes and cumulative risk caused by a scenario which results in a combination of crash damage, e.g., from rollover and subsequent pool fire. Modeling efforts will establish possible outcomes and be used to identify and select conditions of interest that warrant future testing and/or additional research.

9.2.4 Effects of Rupture

The effects of tank rupture in the presence and absence of a fire will be evaluated to assess threats to first responders.

10. References

ASTM International. (2016). Measuring Heat Flux Using Directional Flame Thermometers with Advanced Data Analysis Techniques. West Conshohocken, PA: ASTM International.

Beck, J. (1999). User's Manual for IHCP1D, a Program for Calculating Surface Heat Fluxes from Transient Temperatures Inside Solids. Okemos, MI: Beck Engineering Consultants Co.

Hurley, M., et al. (2016). Chapter 71: BLEVES and Fireballs. *SFPE Handbook of Fire Protection Engineering* (5th Ed.) (pp. 2806–2807). Gaithersburg, MD: Society of Fire Protection Engineers.

Hyde, D. W. (1988). User's Guide for Microcomputer Programs ConWep and FunPro, Applications of TM 5-855-1. *Fundamentals of Protective Design for Conventional Weapons.* Vicksburg, MS: U.S. Army Engineer Waterways Experiment Station.

Keltner, N., Nash, L., Beitel, J., Parker, A., Welsh, S., and Gilda, B. (2001). Fire Safety Test Furnace Characterization Unit. ASTM STP 1427. In L.A. Gritzo and N. Alvares (Eds.), *Thermal Measurements: The Foundation of Fire Standards* (pp. 128–146). West Conshohocken, PA: ASTM International.

Martinez, J. M. B. (2011, October). Liquefied Natural Gas Road Tanker Explosion. Internal Report, Murcia Fire Service & Rescue.

Planas, E., et al. (2015). Analysis of the BLEVE of a LNG road tanker: The Zarzalico accident. *Journal of Loss Prevention in the Process Industries, 34,* 127–138.

Planas-Cuchi, E., Gasulla, N., Ventosa, A., and Casal, J. (2004). Explosion of a Road Tanker Containing Liquefied Natural Gas. *Journal of Loss Prevention in the Process Industries, 17,* 315–321.

Raj, P. (2006). LNG fires: A review of experimental results, models and hazard prediction challenges. *Journal of Hazardous Materials, 140,* 444–464.

Stroup, D., Taylor, G., and Hausman, G. (2013). Fire Dynamics Tools (FDTs) Quantitative Fire Hazard Analysis Methods for the U.S. Nuclear Regulatory Commission Fire Protection Inspection Program (NUREG-1805, Supplement 1, Volumes 1 & 2). Washington, DC: U.S. Nuclear Regulatory Commission.

Appendix A.
CVA ISO Storage Tank Drawings

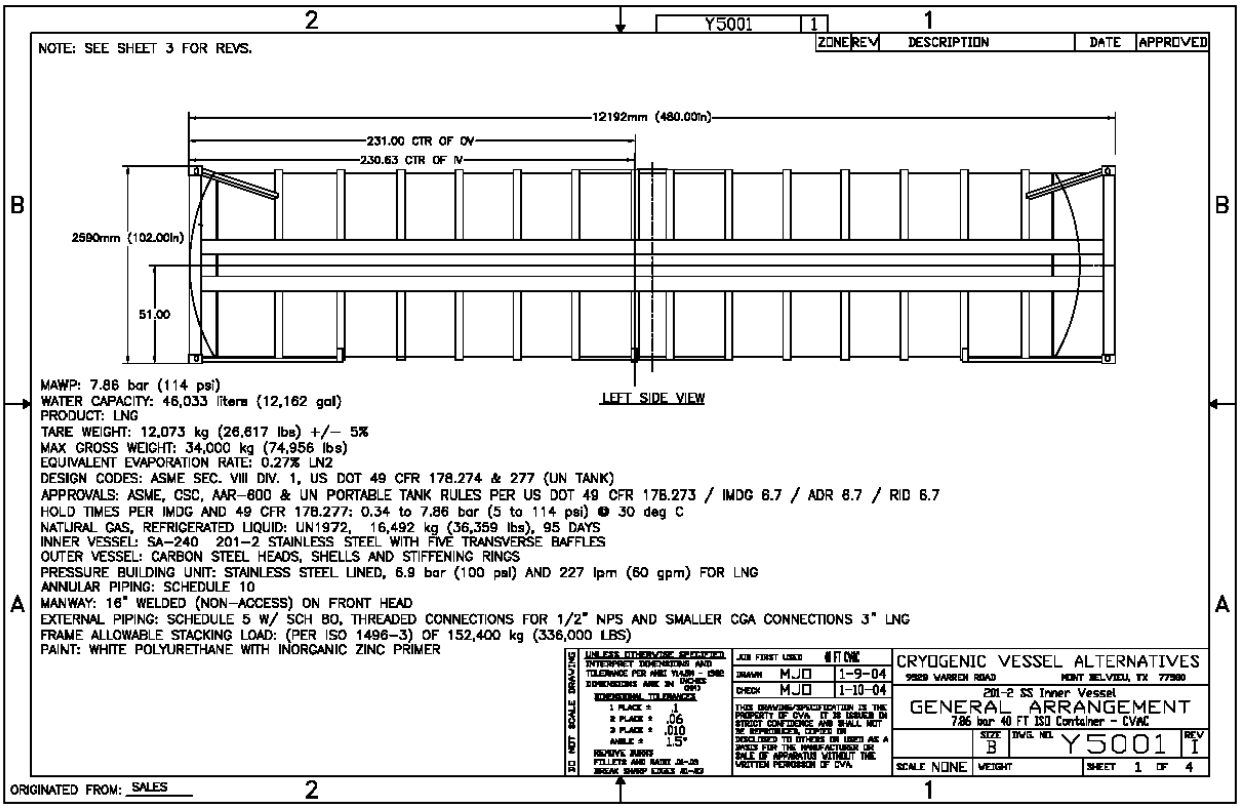

Figure A-1: **General Arrangement (left side) of CVA ISO storage Tank**

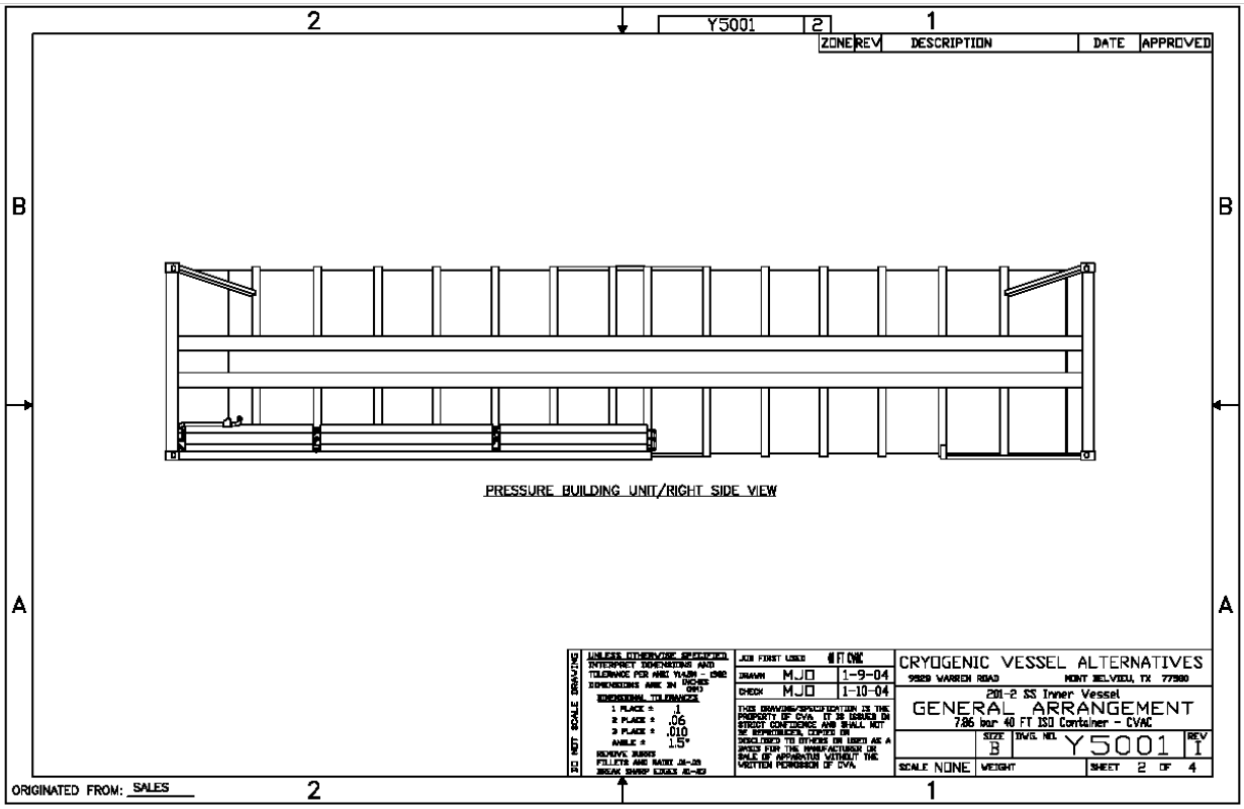

Figure A-2: General Arrangement (right side) of CVA ISO storage Tank

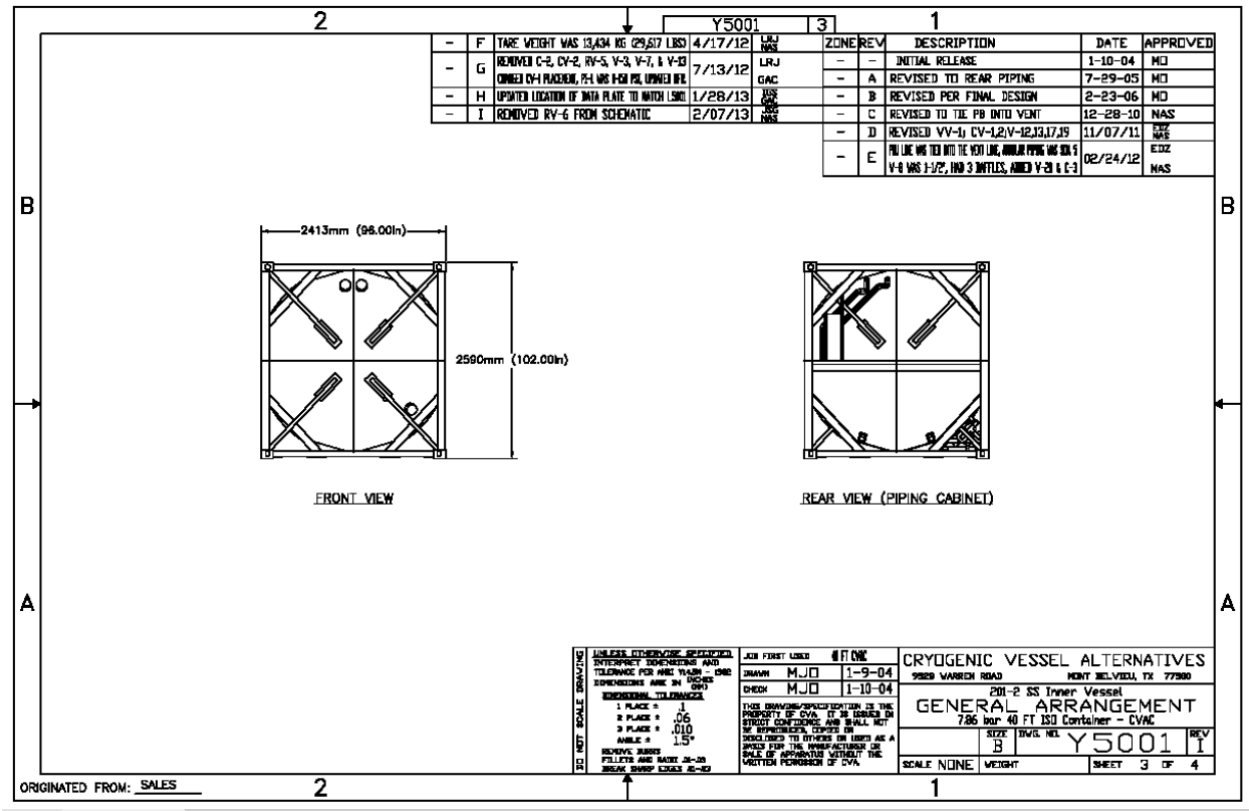

Figure A-3: General Arrangement (front and rear sides) of CVA ISO Storage Tank

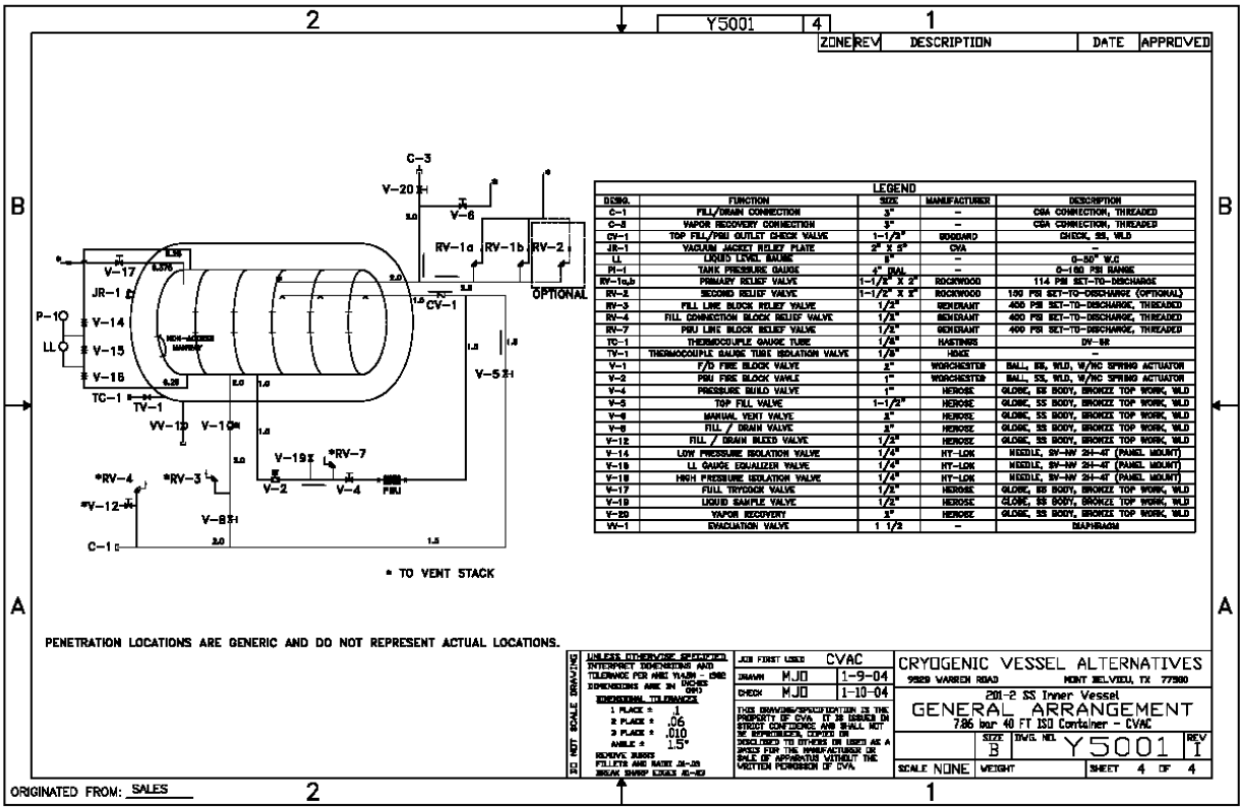

DSNG.	FUNCTION	SIZE	MANUFACTURER	DESCRIPTION
C-1	FILL/DRAIN CONNECTION	3"	–	CGA CONNECTION, THREADED
C-2	VAPOR RECOVERY CONNECTION	3"	–	CGA CONNECTION, THREADED
CV-1	TOP FILL/PRU OUTLET CHECK VALVE	1-1/2"	GOODARD	CHECK, SS, WLD
JR-1	VACUUM JACKET RELIEF PLATE	2" X 5"	CVA	–
LL	LIQUID LEVEL GAUGE	8"	–	0-50" W.C
PI-1	TANK PRESSURE GAUGE	4" DIAL	–	0-160 PSI GAUGE
RV-1a,b	PRIMARY RELIEF VALVE	1-1/2" X 2"	ROCKWOOD	114 PSI SET-TO-DISCHARGE
RV-2	SECOND RELIEF VALVE	1-1/2" X 2"	ROCKWOOD	120 PSI SET-TO-DISCHARGE (OPTIONAL)
RV-3	FILL LINE BLOCK RELIEF VALVE	1/2"	SENTRANT	400 PSI SET-TO-DISCHARGE, THREADED
RV-4	FILL CONNECTION BLOCK RELIEF VALVE	1/2"	SENTRANT	400 PSI SET-TO-DISCHARGE, THREADED
RV-7	PRU LINE BLOCK RELIEF VALVE	1/2"	SENTRANT	400 PSI SET-TO-DISCHARGE, THREADED
TC-1	THERMOCOUPLE GAUGE TUBE	1/8"	HASTINGS	DV-6R
TV-1	THERMOCOUPLE GAUGE TUBE ISOLATION VALVE	1/8"	HOKE	–
V-1	F/D FIRE BLOCK VALVE	2"	WORCHESTER	BALL, SS, WLD, W/NO SPRING ACTUATOR
V-2	PRU FIRE BLOCK VAHLE	1"	WORCHESTER	BALL, SS, WLD, W/NO SPRING ACTUATOR
V-4	PRESSURE BUILD VALVE	1"	HENOSE	GLOBE, SS BODY, BRONZE TOP WORK, WLD
V-5	TOP FILL VALVE	1-1/2"	HENOSE	GLOBE, SS BODY, BRONZE TOP WORK, WLD
V-6	MANUAL VENT VALVE	3"	HENOSE	GLOBE, SS BODY, BRONZE TOP WORK, WLD
V-8	FILL / DRAIN VALVE	3"	HENOSE	GLOBE, SS BODY, BRONZE TOP WORK, WLD
V-12	FILL / DRAIN BLEED VALVE	1/2"	HENOSE	GLOBE, SS BODY, BRONZE TOP WORK, WLD
V-14	LOW PRESSURE ISOLATION VALVE	1/4"	HY-LOK	NEEDLE, SV-NW 24-4T (PANEL MOUNT)
V-15	LL GAUGE EQUALIZER VALVE	1/4"	HY-LOK	NEEDLE, SV-NW 24-4T (PANEL MOUNT)
V-16	HIGH PRESSURE ISOLATION VALVE	1/4"	HY-LOK	NEEDLE, SV-NW 24-4T (PANEL MOUNT)
V-17	FULL TRYCOCK VALVE	1/8"	HENOSE	GLOBE, SS BODY, BRONZE TOP WORK, WLD
V-19	LIQUID SAMPLE VALVE	1/2"	HENOSE	GLOBE, SS BODY, BRONZE TOP WORK, WLD
V-20	VAPOR RECOVERY	1"	HENOSE	GLOBE, SS BODY, BRONZE TOP WORK, WLD
VV-1	EVACUATION VALVE	1 1/2	–	DIAPHRAGM

Figure A-4: Piping Arrangement of CVA ISO storage Tank

Appendix B.
Instrumentation Drawings

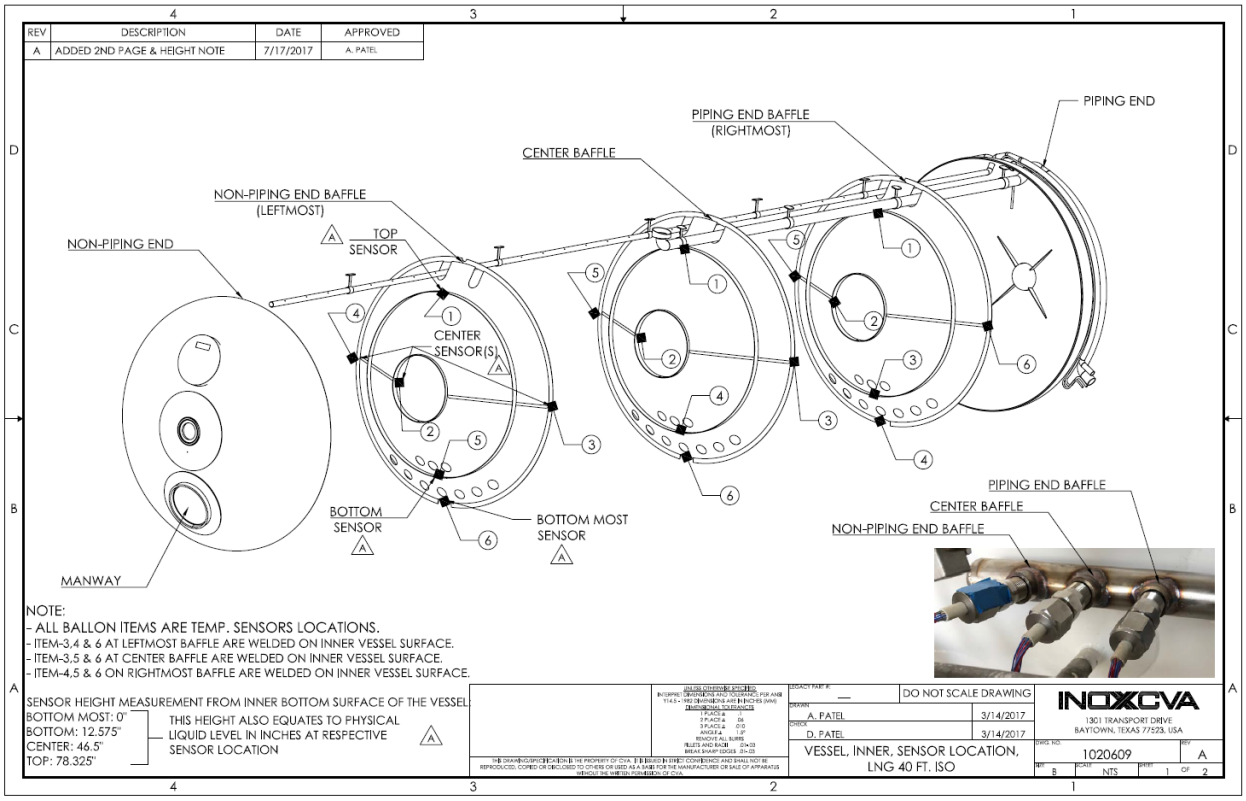

Figure B-1: Arrangement of Thermocouple Trees in Inner Tank (provided by CVA)

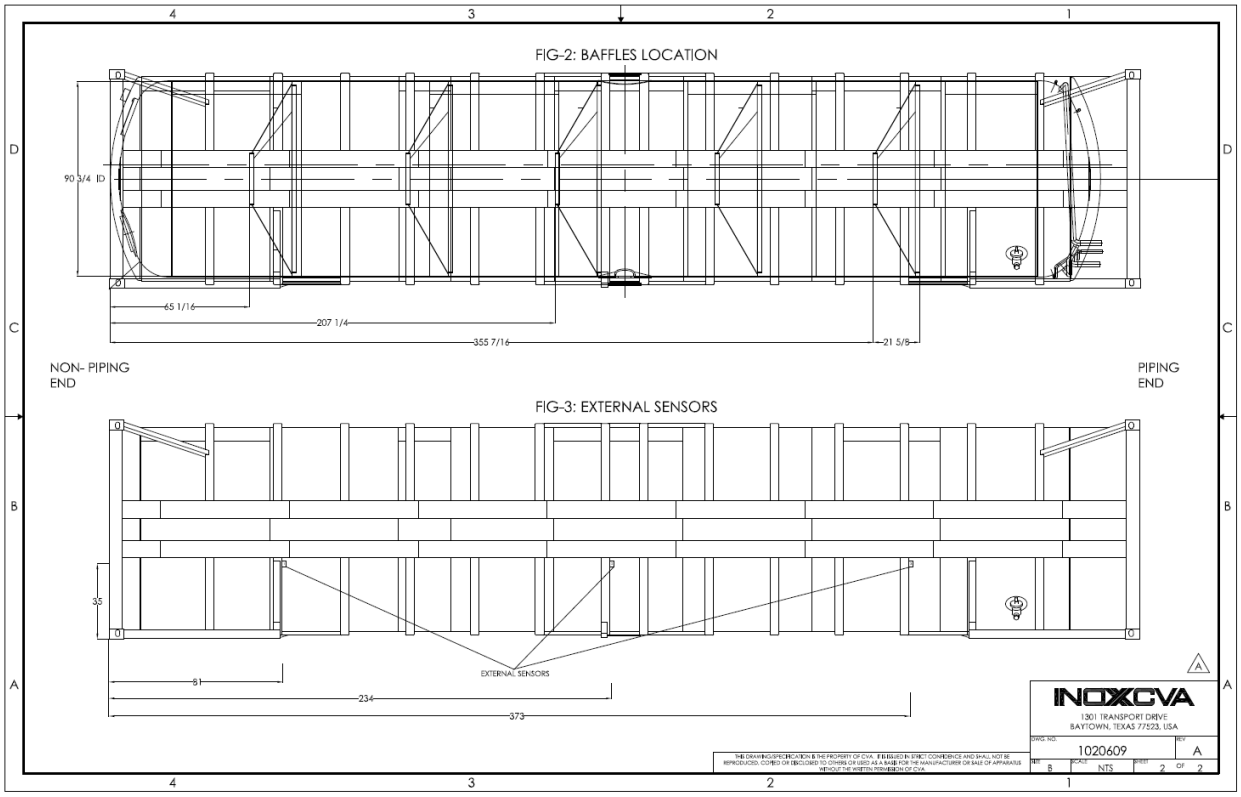

Figure B-2: ISO Tank Showing Location of Baffles in Plain View and External Weld-Pad Thermocouples in Elevation View (provided by CVA)

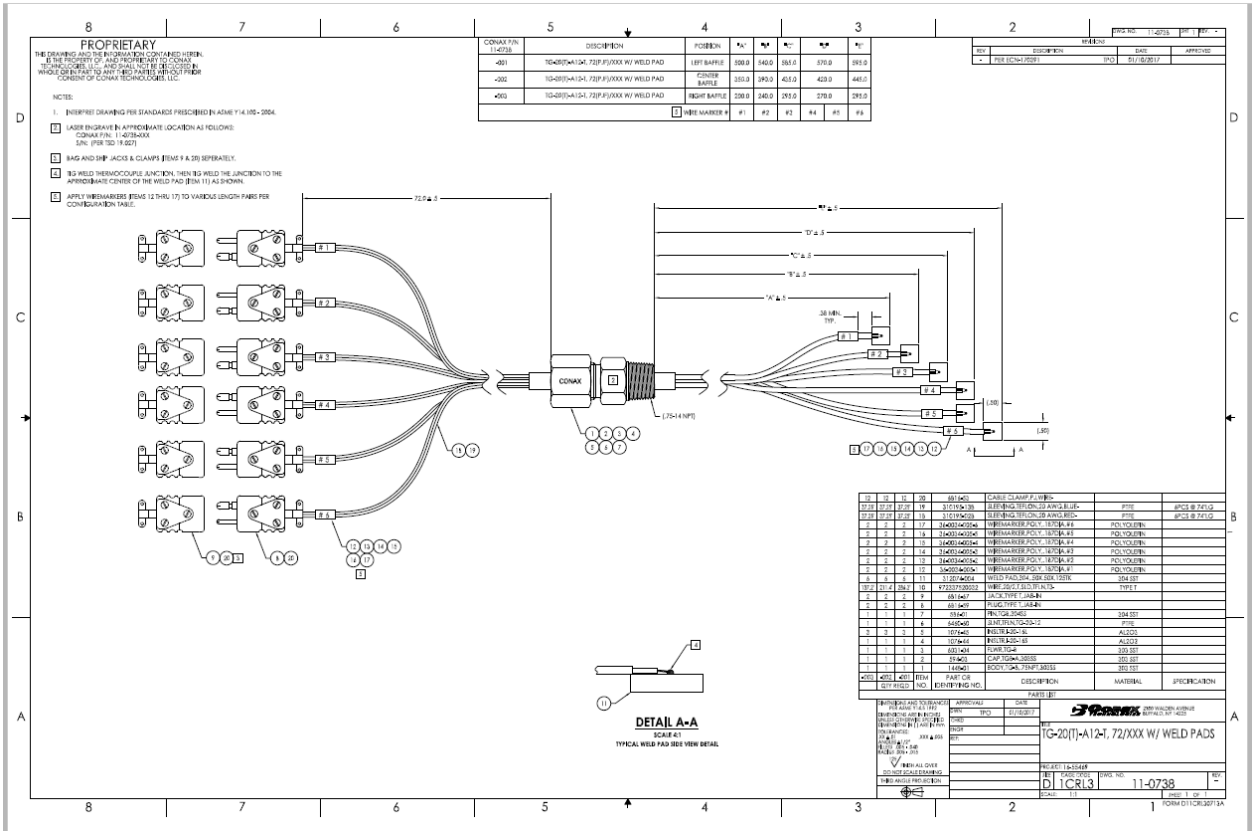

Figure B-3: **Internal Temperature Pass-Through Connector Drawing**

Abbreviations and Acronyms

ACRONYMS	EXPLANATION
AAR	Association of American Railroads
BLEVE	Boiling Liquid Expanding Vapor Explosion
CFD	Computational Fluid Dynamics
CNG	Compressed Natural Gas
CVA	Cryogenic Vessel Alternatives, Inc.
DAQ	Data Acquisition System
DFT	Directional flame thermometer
DOT	Department of Transportation
FRA	Federal Railroad Administration
FE	Finite Element
FDS	Fire Dynamics Simulator
FECR	Florida East Coast Railway
FRC	Freidman Research Corporation
GHG	Greenhouse Gasses
HRRPUA	Heat Release Rate Per Unit Area
ISO	International Organization for Standardization
LNG	Liquefied Natural Gas
LPG	Liquefied Petroleum Gas
LN2	Liquid Nitrogen
NIST	National Institute of Science and Technology
OSHA	Occupational Safety and Health Administration
PRV	Pressure Relief Valve
SwRI	Southwest Research Institute
TAG	Technical Advisory Group
TC	Thermocouple
VTT	Valtion Teknillinen Tutkimuskeskus